

Ice-marginal forced regressive deltas in glacial lake basins: geomorphology, facies variability and large-scale depositional architecture

JUTTA WINSEMANN , JÖRG LANG, ULRICH POLOM, MARKUS LOEWER, JAN IGEL, LUKAS POLLOK AND CHRISTIAN BRANDES

BOREAS



Winsemann, J., Lang, J., Polom, U., Loewer, M., Igel, J., Pollok, L. & Brandes, C. 2018 (October): Ice-marginal forced regressive deltas in glacial lake basins: geomorphology, facies variability and large-scale depositional architecture. *Boreas*, Vol. 47, pp. 973–1002. <https://doi.org/10.1111/bor.12317>. ISSN 0300-9483.

This study presents a synthesis of the geomorphology, facies variability and depositional architecture of ice-marginal deltas affected by rapid lake-level change. The integration of digital elevation models, outcrop, borehole, ground-penetrating radar and high-resolution shear-wave seismic data allows for a comprehensive analysis of these delta systems and provides information about the distinct types of deltaic facies and geometries generated under different lake-level trends. The exposed delta sediments record mainly the phase of maximum lake level and subsequent lake drainage. The stair-stepped profiles of the delta systems reflect the progressive basinward lobe deposition during forced regression when the lakes successively drained. Depending on the rate and magnitude of lake-level fall, fan-shaped, lobate or more digitate tongue-like delta morphologies developed. Deposits of the stair-stepped transgressive delta bodies are buried, downlapped and overlapped by the younger forced regressive deposits. The delta styles comprise both Gilbert-type deltas and shoal-water deltas. The sedimentary facies of the steep Gilbert-type delta foresets include a wide range of gravity-flow deposits. Delta deposits of the forced-regressive phase are commonly dominated by coarse-grained debrisflow deposits, indicating strong upslope erosion and cannibalization of older delta deposits. Deposits of supercritical turbidity currents are particularly common in sand-rich Gilbert-type deltas that formed during slow rises in lake level and during highstands. Foreset beds consist typically of laterally and vertically stacked deposits of antidunes and cyclic steps. The trigger mechanisms for these supercritical turbidity currents were both hyperpycnal meltwater flows and slope-failure events. Shoal-water deltas formed at low water depths during both low rates of lake-level rise and forced regression. Deposition occurred from tractional flows. Transgressive mouthbars form laterally extensive sand-rich delta bodies with a digitate, multi-tongue morphology. In contrast, forced regressive gravelly shoal-water deltas show a high dispersion of flow directions and form laterally overlapping delta lobes. Deformation structures in the forced-regressive ice-marginal deltas are mainly extensional features, including normal faults, small graben or half-graben structures and shear-deformation bands, which are related to gravitational delta tectonics, postglacial faulting during glacial-isostatic adjustment, and crestal collapse above salt domes. A neotectonic component cannot be ruled out in some cases.

Jutta Winsemann (winsemann@geowi.uni-hannover.de), Jörg Lang, Lukas Pollok and Christian Brandes, Institut für Geologie, Leibniz Universität Hannover, Callinstr. 30, 30167 Hannover, Germany; Ulrich Polom, Markus Loewer and Jan Igel, Leibniz Institute for Applied Geophysics (LIAG), Stilleweg 2, D-30655 Hannover, Germany; Lukas Pollok, Bundesanstalt für Geowissenschaften und Rohstoffe (BGR), Stilleweg 2, D-30655 Hannover, Germany; received 16th August 2017, accepted 27th February 2018.

Ice-marginal deltas are excellent palaeogeographical archives, recording the glaciation history of marine and continental basins. These deltas commonly evolve from ice-contact systems to glacialfluvial deltas during ice-margin stillstand and retreat (Lønne 1995; Dietrich *et al.* 2017) and delta foreset–topset contacts can be used as water-level indicators if shoreline features are poorly developed or became eroded by later peri- and paraglacial processes (Winsemann *et al.* 2009, 2011; Perkins & Brennand 2015; Lang *et al.* 2018). In remote areas delta morphology and the dimensions of feeder channels can be used as an important record of palaeo-lakes and the magnitude of surface-water flow (Martin & Jansson 2011; Villiers *et al.* 2013).

The depositional architecture of delta systems is a sensitive archive of short- and long-term base-level changes and many delta studies during the last 20 years focussed on a sequence- stratigraphic interpretation of marine systems and their response to global sea-level change (Postma 1995; Posamentier & Morris 2000; Uličný 2001; Catuneanu *et al.* 2011). However,

there is still a need for a better understanding of the facies variability, progradation styles and large-scale depositional architecture of forced-regressive ice-marginal depositional systems, which are less well understood compared to non-glacigenic sedimentary environments (Brookfield & Martini 1999; Powell & Cooper 2002; Gutsell *et al.* 2004; Hirst 2012; Lang *et al.* 2012; Nutz *et al.* 2015; Dietrich *et al.* 2017; Gilbert *et al.* 2017).

This study presents a synthesis of the geomorphology, facies variability and large-scale depositional architecture of ice-marginal deltas controlled by rapid lake-level change. The selected field examples are considered to be representative of delta styles in glacial lake basins. The integration of digital elevation models, outcrop, borehole, ground-penetrating radar (GPR) and high-resolution shear-wave seismic data allow assessment of the role of rapid base-level change in delta morphology, sedimentary facies and the larger-scale depositional architecture. The results are compared with other marine and lacustrine delta examples from the literature, and provide information about the distinct types

of deltaic facies and geometries generated under different lake-level trends, helping to recognize a hidden record of such changes where deltaic systems are poorly exposed.

Delta styles and depositional processes

Gilbert-type ice-marginal deltas commonly reflect a relatively stable position of the ice-margin in front of mountain ranges or bedrock highs that acted as pinning points (Powell 1990; Ashley 1995; Lønne 1995; Winsemann *et al.* 2007, 2011; Girard *et al.* 2015). If the ice terminus remains stable for a longer period of time, grounding line fans may also aggrade to lake level and form an ice-contact/glacifluvial delta (Powell 1990; Lønne 1995). Shoal-water ice-marginal deltas may form in low-gradient settings along lake-basin strike, during lake-level rise on drowned Gilbert-type delta plains, or during lake-level fall (Ashley 1995; Winsemann *et al.* 2009; Eilertsen *et al.* 2011). The sediment supply is dominated by ephemeral meltwater flows from glaciers and massflows from hill slopes whereby the sediment yield from hill slopes strongly depends upon the local availability of (melt)water. In glaciolacustrine environments, the sediment-laden meltwater is typically denser than the surrounding lake water and the deposition on delta slopes is therefore likely to be dominated by a wide range of gravity flows, with comparatively minor inputs from high-level suspended sediment (Ashley 1995; Lønne & Nemeč 2004; Winsemann *et al.* 2011).

The depositional processes in coarse-grained ice-marginal deltas have been discussed in many studies (Ashley 1995; Lønne 1995; Nemeč *et al.* 1999; Plink-Björklund & Ronnert 1999; Lønne & Nemeč 2004; Winsemann *et al.* 2007, 2011; Ghienne *et al.* 2010; Eilertsen *et al.* 2011; Girard *et al.* 2012; Dietrich *et al.* 2016). However, the interpretation of gravity-flow deposits has considerably changed during recent years and recently the deposition by supercritical density flows has become a major focus of research, changing previous views (Postma *et al.* 2009; Postma & Cartigny 2014; Postma *et al.* 2014). Related bedforms on the delta slope include deposits of antidunes, chutes-and-pools and cyclic steps, which might be partly misinterpreted as scour fills or wave-induced hummocky cross-stratification (cf. Fielding 2006; Muto *et al.* 2012; Lang & Winsemann 2013; Cartigny *et al.* 2014; Postma *et al.* 2014; Dietrich *et al.* 2016; Massari 2017; Lang *et al.* 2017a, b). Deposits of supercritical density flows may record high-magnitude (glacial) floods (Ghienne *et al.* 2010; Winsemann *et al.* 2011; Girard *et al.* 2012, 2015; Carling 2013; Ventra *et al.* 2015) or represent delta slope failure events producing slides, slumps, debrisflows and/or turbidity currents (Talling 2014; Dietrich *et al.* 2016; Hughes Clarke 2016).

The complex morphology and depositional architecture of delta systems are the result of an interplay of

water discharge, sediment supply and available accommodation space (Dunne & Hempton 1984; Postma 1995; Posamentier & Morris 2000; Muto & Steel 2001, 2004; Uličný 2001; Lønne & Nemeč 2004; Ritchie *et al.* 2004a, b; Petter & Muto 2008; Eilertsen *et al.* 2011; Winsemann *et al.* 2011; Gobo *et al.* 2014, 2015). The geological setting and type of dam exert key controls on proglacial lake growth and drainage. Major controlling factors are the location of the ice margin, elevation and topography of the surrounding landscape and the location and elevation of the lake-overflow channel(s) (Teller 1987; Kehew & Teller 1994; Carrivick & Tweed 2013; Lang *et al.* 2018). In contrast to glaciomarine settings, glacial lake basins are typically characterized by an initial base-level rise during glacier advance, as the glacier blocks drainage outlets. Forced regression characteristically occurs during deglaciation when lake outlets are opened and rapid lake-level falls may occur (Kehew & Teller 1994; Ashley 1995; Brookfield & Martini 1999; Winsemann *et al.* 2011; Carrivick & Tweed 2013; Winsemann *et al.* 2016).

The depositional architecture of delta systems is therefore a sensitive archive of short- and long-term base-level changes (Fig. 1), with the formation of delta-brink rising trajectories during base-level rise and delta-brink subhorizontal or falling trajectories during base-level stillstand and fall (Posamentier & Morris 2000; Catuneanu *et al.* 2011; Gobo *et al.* 2015). During transgression, the high rates of lake-level rise, which are common in glacial lake basins (Oviatt *et al.* 1992; Winsemann *et al.* 2011), will cause a rapid landward shift of delta-front lobes (Posamentier & Morris 2000; Catuneanu *et al.* 2011) and the formation of a stair-stepped delta morphology (Muto & Steel 2001; Ritchie *et al.* 2004b; Villiers *et al.* 2013). Forced regression is defined as basinward shoreline retreat during relative base-level fall, whereas normal regression may occur during the base-level lowstand, rise and highstand, if the sediment supply exceeds the rate at which accommodation space is created (Posamentier & Morris 2000). Alluvial-plain aggradation and delta-front progradation commonly accompany normal regression, whereas fluvial incision and sediment bypass occur during forced regression (Posamentier & Morris 2000; Ritchie *et al.* 2004a, b; Strong & Paola 2008; Catuneanu *et al.* 2011), leading to a rapid basinward stepping of delta lobes (Fig. 1). A possible genetic link between the delta-front morphodynamic responses to base-level changes and the delta-slope sedimentation processes may help in the recognition of a hidden record of base-level change if the topset–foreset transition zone is eroded (Gobo *et al.* 2014, 2015).

Study area

The study area is located south of the North German Lowlands (Fig. 2). Luminescence data of ice-marginal deposits (Roskosch *et al.* 2015; Lang *et al.* 2018) point to several ice advances into this area during the Middle

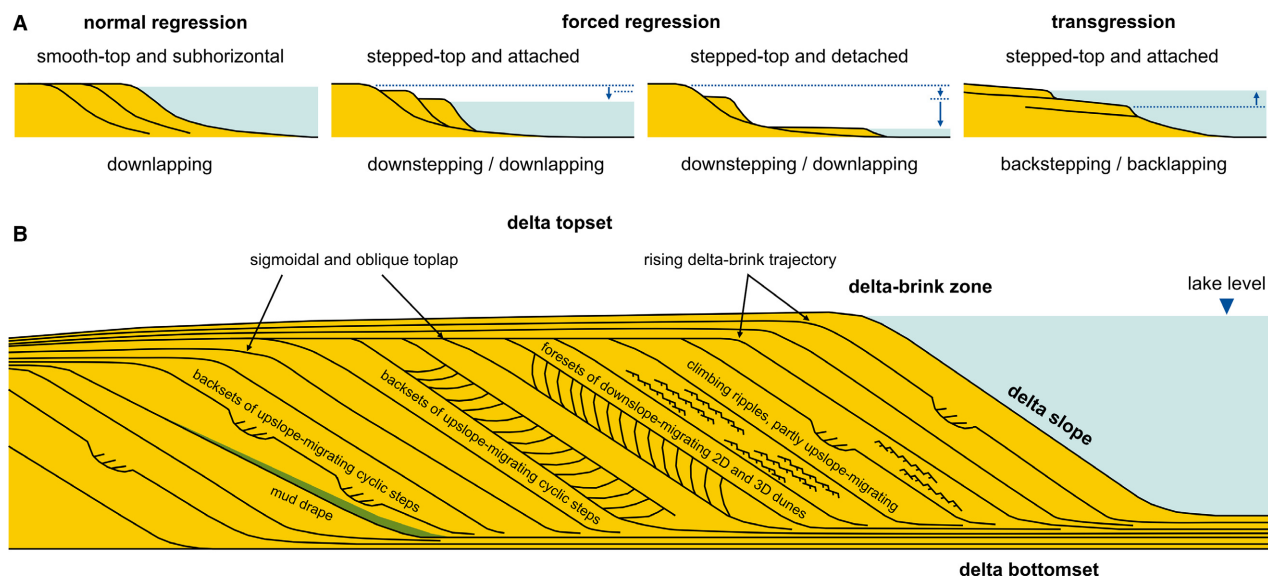


Fig. 1. Schematic longitudinal cross-section of a Gilbert-type delta, showing characteristic architectural features and stratal stacking patterns (compiled and modified from Posamentier & Morris 2000; Catuneanu *et al.* 2011; Gobo *et al.* 2014 and Lang *et al.* 2017b). [Colour figure can be viewed at www.boreas.dk]

Pleistocene (Marine Isotope Stages MIS 12 to 6). The blocking of river valleys by the Middle Pleistocene Elsterian and Saalian ice sheets led to the repetitive formation of proglacial lakes (Eissmann 2002; Winsemann *et al.* 2007, 2009; Roskosch *et al.* 2015; Lang *et al.* 2018). These proglacial lakes were characterized by overall water rises during ice advances, when lake-overspill channels were successively closed. Maximum lake levels of ~200 m a.s.l. were reached during the Saalian glaciation, with lake-level rises of up to 150 m within a few hundreds to thousand years (Winsemann *et al.* 2011; Lang *et al.* 2018). During deglaciation, the lakes catastrophically drained due to the renewed opening of lake outlets, which caused rapid, high-magnitude lake-level falls in the range of 20–80 m within perhaps a few weeks (Meinsen *et al.* 2011; Winsemann *et al.* 2011, 2016; Lang *et al.* 2018). The lake-level history of glacial lakes along the Elsterian ice-sheet margins (MIS 12 and 10) in northern central Europe is less well studied. The maximum lake levels in eastern Germany were probably similar to those of the Saalian glaciation, controlled by the topographic height of lake-overspill channels (Lang *et al.* 2018). The Elsterian lake levels of glacial Lake Leine probably reached ~155 m a.s.l. (Roskosch *et al.* 2015), corresponding to a lake-level rises of approximately 80 m. Estimated lake-level falls during deglaciation were in the range of 20–25 m. It is not known if larger glacial lakes existed in the Weser Valley during the Elsterian glaciations.

The ice-marginal delta systems are relatively small, ranging in size from ~1.5 to ~5 km². Their thickness varies between ~35 and ~70 m. The Gilbert-type deltas are commonly located in front of steep mountain ridges and are fed by bedrock-feeder channels (Winsemann *et al.* 2007, 2011). In some cases, subaqueous ice-contact fans

are downlapped, overlapped or overlain by Gilbert-type delta systems and/or shoal-water deltas (Winsemann *et al.* 2009). New outcrops reveal the presence of abundant bedforms deposited by supercritical density flows (Lang *et al.* 2017b). Gravelly shoal-water deltas formed during lake-level fall when water depths became low (Roskosch *et al.* 2015).

Methodology

Geomorphology and sedimentology of delta systems

High-resolution digital elevation models (10-m grid, vertical resolution: ± 0.5 m) were analysed in a geographical information system (ArcGIS). The geomorphology of the Freden delta has been reconstructed from old topographic maps (1901/1937) with ArcGIS software (3ArcGIS Version 10.3.1, Esri, Redlands, CA, USA).

Outcrop and borehole data were studied to reconstruct the sedimentary facies and depositional architecture of ice-marginal delta systems. Vertical logs were measured at the scale of individual beds, noting grain size, bed thickness, bed contacts, bed geometry, internal sedimentary structures and palaeocurrent directions. Photomosaics of larger outcrops were used for the interpretation of architectural elements. The terminology for gravel characteristics is after Walker (1975).

Ground-penetrating radar profiles

Ground-penetrating radar (GPR) was used to delineate architectural elements. These data provide a bridge between outcrop-facies architecture and the larger-scale

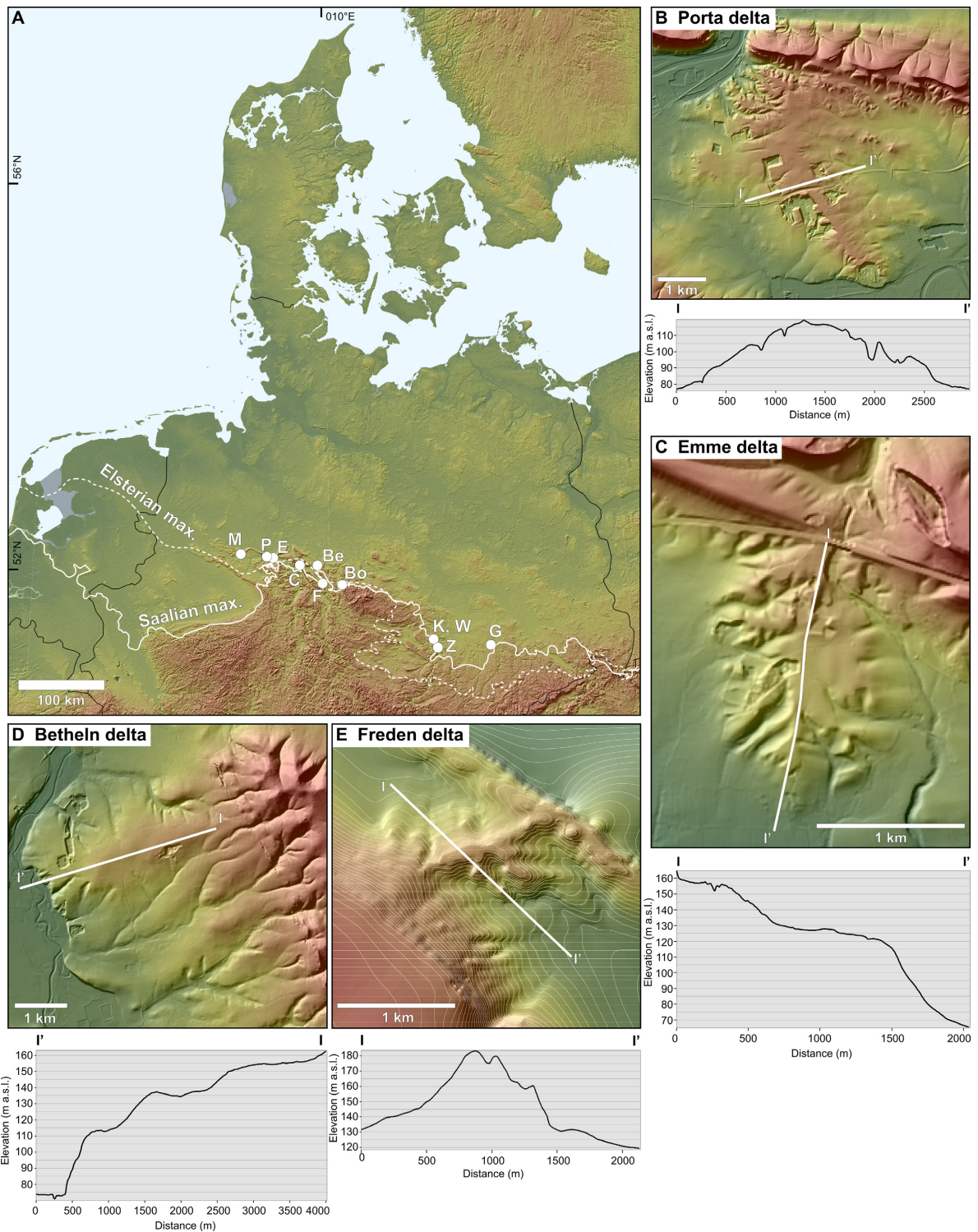


Fig. 2. Location and topography of the study area. A. Maximum extent of the Middle Pleistocene Elsterian and Saalian ice sheets in central Europe and associated ice-marginal delta systems. Data are compiled from Winsemann *et al.* (2007, 2009, 2011) and Lang *et al.* (2018). The DEM is based on Copernicus data and information funded by the European Union (EU-DEM layers). Be = Betheln delta; Bo = Bornhausen delta; C = Copenbrügge subaqueous fan and delta complex; E = Emme delta; F = Freden delta; G = Großsteinberg delta; K = Karsdorf delta; M = Markendorf delta; P = Porta subaqueous fan and delta complex; W = Wunsch delta; Z = Zeuchfeld delta. B–E. Geomorphology of the Porta subaqueous fan and delta complex, Emme delta, Betheln delta and Freden delta. Geomorphological profiles (I–I') are shown below each delta map. The DEMs of the Porta subaqueous fan and delta complex, Emme delta and Betheln delta are based on data from the Bezirksregierung Köln (10-m grid, vertical resolution: ± 0.5 m) and LGN Hannover (10-m grid, vertical resolution: ± 0.5 m). The DEM of the Freden delta is reconstructed from old topographic maps (1901/1937) with ArcGIS software. Contour lines are in 5-m intervals. [Colour figure can be viewed at www.boreas.dk]

delta architecture mapped from shear-wave seismic profiles. The GPR device used was a GSSI SIR-3000 (Geophysical Survey Systems Inc. (GSSI), Nashua, NH, USA) with 200 and 400 MHz shielded antennas. Radar traces were collected every 5 cm along the profile and the data processing comprised dewowing, static correction, amplitude balancing by spherical divergence compensation and application of an exponential gain function, bandpass filtering and migration. The vertical resolution is ~5–10 cm. The lateral resolution is ~30–50 cm near the surface and ~0.8–1.1 m at 5-m depth. The radar facies were defined on the basis of the external geometry and the internal reflector patterns (Gutsell *et al.* 2004; Neal 2004; Lee *et al.* 2007; Eilertsen *et al.* 2011).

Shear-wave seismic profiles

The larger-scale delta architecture was mapped from high-resolution shear-wave seismic profiles. The vertical resolution is up to ~0.5 m. The lateral resolution is about 0.5 m near the surface and decreases to ~12 m at 50-m depth. For all surveys presented here we combined a shear-wave land streamer with the micro-vibrator ELVIS (developed by LIAG) operating in transverse horizontal (SH) mode. Details on data acquisition and processing are given in Winsemann *et al.* (2011) and Roskosch *et al.* (2015).

The seismic facies were defined on the basis of the external geometry and internal reflector patterns (Mitchum *et al.* 1977; Posamentier & Vail 1988). The seismic attributes amplitude and continuity were used for the analysis of reflector patterns (Bullimore *et al.* 2005).

Geomorphology and large-scale depositional architecture of delta systems

Four delta complexes were selected for this study, referred to as the Porta delta, Emme delta, Betheln delta and Freden delta (Fig. 2A–E). These selected field cases are considered to be representative of the delta styles in glacial lake basins affected by rapid base-level change.

The Porta delta

The Saalian Porta subaqueous fan and delta complex is located at the northern margin of glacial Lake Weser. It has a bedrock-feeder channel, is approximately 6.2 km long and 5.3 km wide and has a radial lobate shape (Fig. 2A, B). The delta system downlaps and onlaps the truncated subaqueous ice-contact fan subaqueous ice-contact fan (Winsemann *et al.* 2009). On top of the truncated fan, a broad glacifluvial delta plain and shallow-water delta mouthbars developed, which fed the marginal Gilbert-type deltas (Fig. 3A; Winsemann *et al.* 2009; Lang *et al.* 2017b). The Porta delta complex is up to ~40 m thick and has a stair-stepped profile with

two plains at ~115 m and ~95 m a.s.l. (Fig. 2B). It formed during an overall lake-level fall, punctuated by lower-magnitude lake-level fluctuations.

The Emme delta

The Saalian Emme delta is located at the northern margin of glacial Lake Weser. It has a deep bedrock-feeder channel, a radial, lobate shape and is about 2 km long, 1.8 km wide and up to 70 m thick (Fig. 2A, C). Luminescence ages point to a deposition during MIS 6 (Lang *et al.* 2018). It overlies glaciolacustrine mud or Jurassic bedrock, forming a concave ramp, dipping at up to 13°. It has a stair-stepped profile with two plains at ~128 m and ~155 m a.s.l. The northeastern upper portion of the delta is characterized by a central, trumpet-shaped, up to 20-m-deep valley that rapidly shallows down-slope. The proximal valley has a sharp, steep western margin that can be traced for ~500 m. In contrast, the eastern valley margin is less well developed and the valley opens rapidly towards the southeast. In front of this incised valley, depositional lobes with a telescoping morphology are developed. The margin of the Emme delta complex displays a radial pattern of ridges and smaller erosional valleys (Fig. 2C). The deposits of the Emme delta record one major transgressive–regressive cycle, punctuated by lower-magnitude lake-level fluctuations (Winsemann *et al.* 2011). The oldest depositional units record the transgressive phase and are characterized by back-stepping delta bodies, decreasing upwards in grain size, thickness and lateral extent (Fig. 3B, seismic units 1–4). During a subsequent series of lake-level falls forced-regressive basinward stepping delta lobes formed that overlie and downlap the transgressive deposits (Fig. 3B, seismic units 5–9).

The Betheln delta

The Elsterian Betheln delta is located at the southwestern slope of the Hildesheimer Wald Mountains (Fig. 2A, D) and has been deposited into glacial Lake Leine. Luminescence ages point to a deposition during MIS 12 (Roskosch *et al.* 2015). The fan-shaped, radial sediment body is about 3.5 km long, 1.5 km wide and up to 35 m thick. It overlies glaciolacustrine mud or Mesozoic bedrock, forming a ramp inclined at up to 6°. The feeder system consists of several parallel bedrock channels (Fig. 2D). The delta has a stair-stepped profile with three marked plains at ~115, ~135 and ~155 m a.s.l. (Fig. 2D). The margin of the delta displays a radial pattern of ridges and smaller erosional valleys (Fig. 2D). The southwestern margin is eroded by the River Leine. The delta complex formed during two transgressive–regressive cycles (Roskosch *et al.* 2015). Deposits of the first transgressive–regressive cycle are characterized by a series of basinward stepping depositional lobes (Fig. 3C, seismic units 1–5), recording the lake-level highstand and

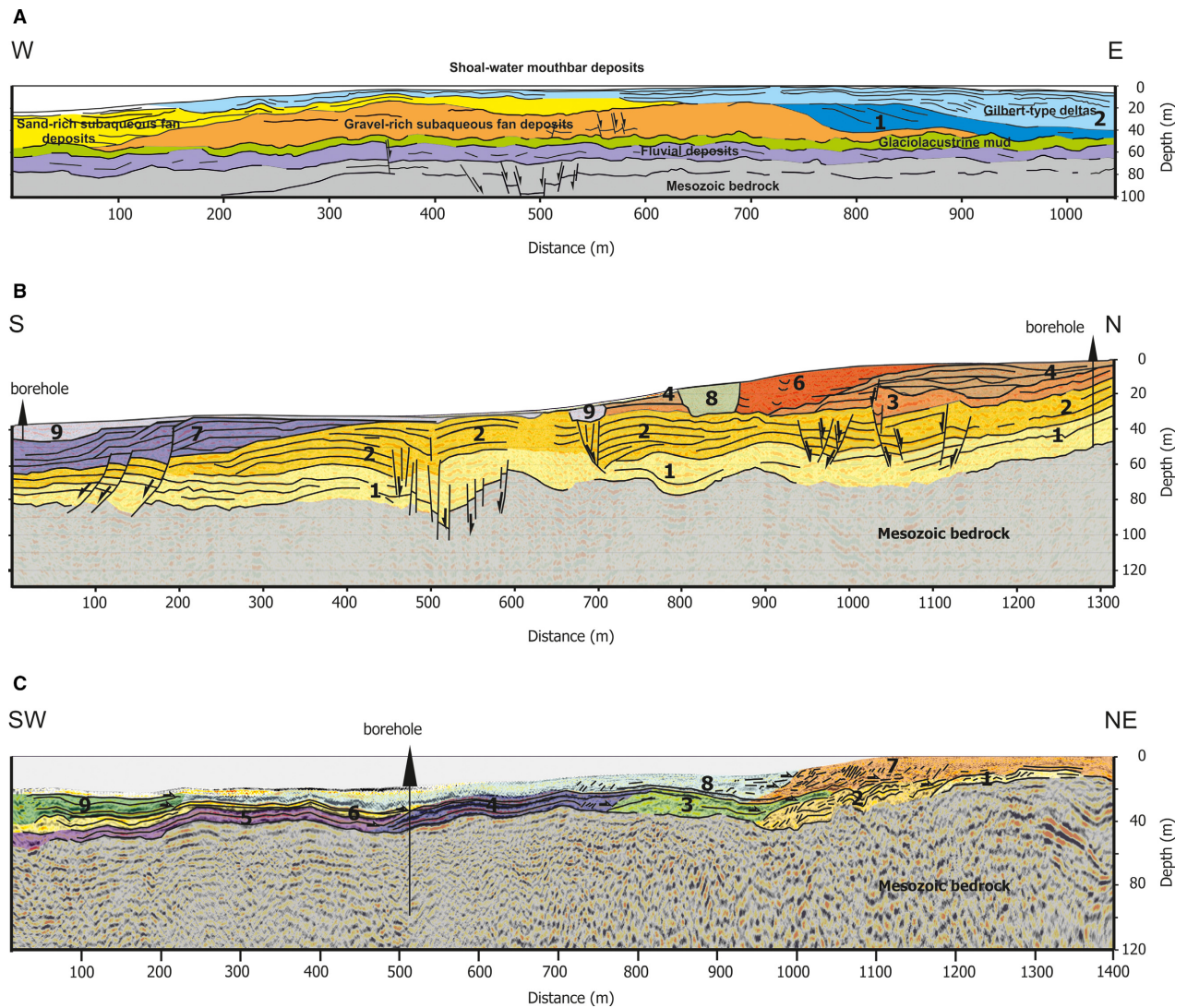


Fig. 3. Shear-wave seismic profiles of the Porta, Emme and Betheln deltas. A. Shear-wave seismic profile of the Porta delta. Two laterally stacked Gilbert-type delta bodies (units 1–2) overlie truncated subaqueous fan deposits. Upslope the younger Gilbert-type delta passes into shallow-water mouthbar deposits (modified from Winsemann *et al.* 2009). B. Shear-wave seismic profile of the Emme delta. The seismic profile shows nine vertically and laterally stacked delta bodies. Delta unit 5 is located southwest of delta unit 2 and not recorded in this line. Two different types of normal fault systems are developed: gravitational normal fault systems restricted to the delta body and normal fault systems that originate in the underlying Mesozoic bedrock and propagate into the overlying delta body (modified from Brandes *et al.* 2011 and Winsemann *et al.* 2011). C. Shear-wave seismic profile of the Betheln delta. The seismic profile shows 10 vertically and laterally stacked delta bodies (extended and modified from Roskosch *et al.* 2015). For Fig. 3B we obtained permission from Wiley. [Colour figure can be viewed at www.boreas.dk]

subsequent lake-level fall. The second transgressive–regressive cycle is represented by seismic units 6–9. During rapid lake-level rise, the older delta units of the first transgressive–regressive cycle were onlapped and overlain by rapidly landward stepping delta lobes (seismic units 6 and 7). During subsequent high-magnitude lake-level falls basinward stepping delta lobes formed that downlap and overlie the older delta deposits (seismic units 8 and 9). The youngest delta units consist of shoal-water mouthbar deltas in the distal portion of the delta complex that downlap the steeply dipping Gilbert-type deltas.

The Freden delta

The Saalian Freden delta is located at the northern margin of glacial Lake Leine. It overlies a salt structure, the so-called Leine anticline (Winsemann *et al.* 2007; Brandes & Tanner 2012), and forms an isolated sediment ridge between two bedrock highs (Fig. 2A, E). This sediment ridge is approximately 1 km wide, 1.5 km long and up to 60 m thick. Towards the northwest, the ice-proximal slope has a concave-up profile inclined at 10° – 2° ; towards the southeast, the delta system has a multi-tongue-like lobate shape with a stair-stepped profile.

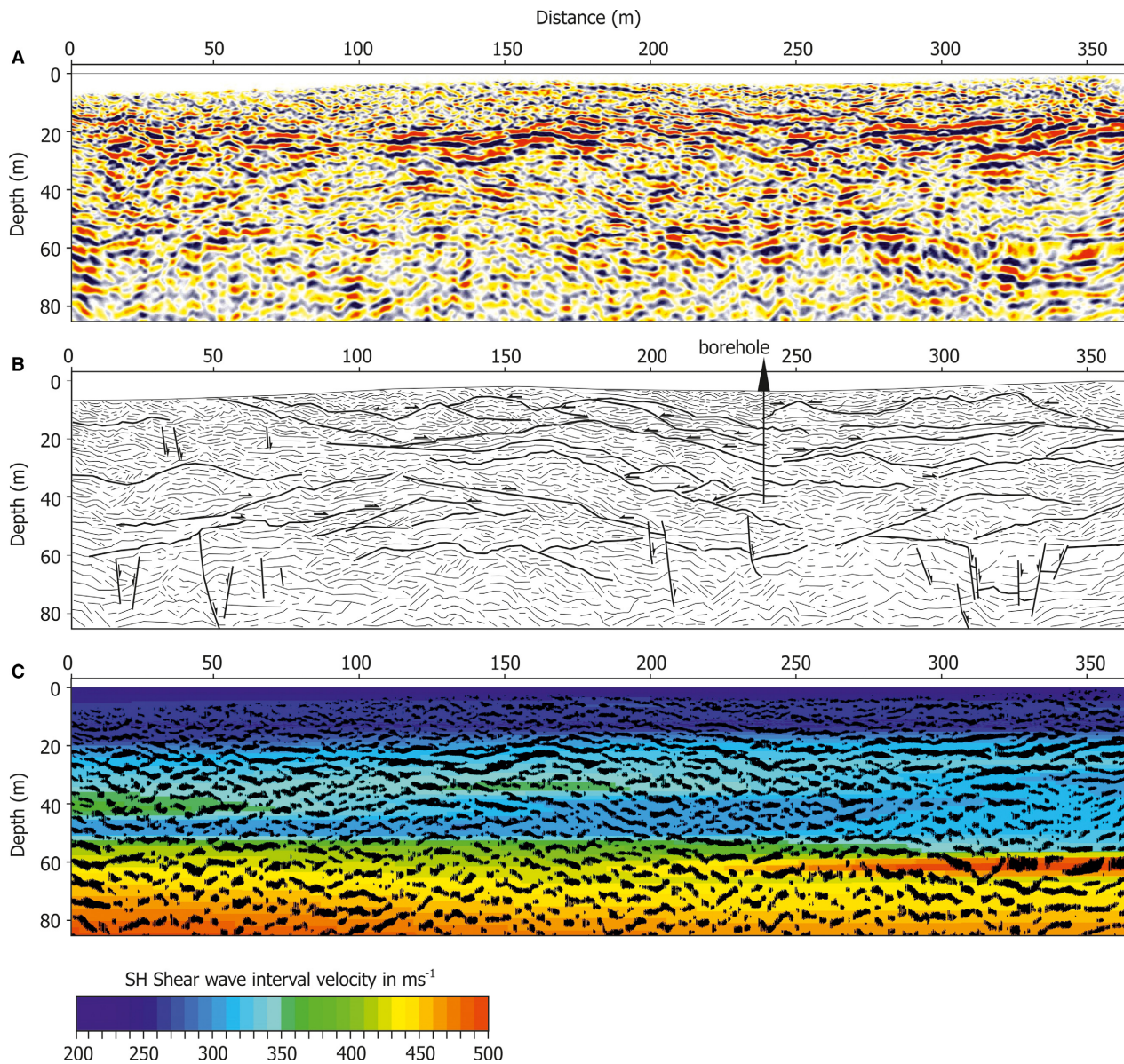


Fig. 4. Shear-wave seismic profile of the Freden delta showing a series of laterally and vertically stacked delta lobes, deposited during overall transgression and lake-level highstand. A. Uninterpreted seismic profile. B. Interpreted seismic profile. C. Velocity coded seismic profile. The shear-wave interval velocity points to three major vertically stacked delta units that differ in velocity. Lower interval velocities and discontinuous, low-amplitude reflectors correlate with coarser-grained sand and pebbly sand. Higher interval velocities and higher amplitude, more continuous reflectors correlate with finer-grained, probably more compacted delta lobe deposits. [Colour figure can be viewed at www.boreas.dk]

Major plains occur at ~180, ~160 and ~130 m a.s.l. (Fig. 2A, E). The depositional architecture points to the existence of two genetically different delta bodies, which are probably related to two transgressive–regressive cycles during MIS 6 and 8 (Roskosch *et al.* 2015). The older sand-rich delta deposits (MIS 8) were probably shed from the northeast via a bedrock feeder channel. The shear-wave seismic line (Fig. 4) shows a series of laterally and vertically stacked depositional lobes that formed during overall transgression. Within these delta deposits numerous shear-deformation bands are developed (Brandes & Tanner 2012; Brandes *et al.* 2018).

During the second ice advance (MIS 6), an ice-contact delta formed in front of an ice lobe that terminated in the lake. These delta deposits contain flow-till layers and glaciotectonic deformation structures, and downlap or unconformably overlie the older delta system (Roskosch *et al.* 2015).

Delta facies associations

The studied deltaic systems comprise Gilbert-type deltas and shoal-water mouthbar deltas. This section summarizes the sedimentary facies associations (FA) and geometrical

features of these delta systems. The delta deposits include a large variety of sedimentary facies (F), representing deposition from low- and high-energy tractional flows, debris fall, debrisflows, and sustained or surge-type supercritical to subcritical turbidity currents. Sediment clasts consist mainly of reworked fluvial material and poorly sorted, angular debris derived from the steep Mesozoic bedrock slopes. Clasts of a Scandinavian/Baltic provenance account for approximately 6–16%. All sedimentary facies (F) are briefly summarized in Table 1; facies associations (FA) are summarized in Table 2.

Gilbert-type deltas (FA1)

The Gilbert-type deltas are characterized by steeply dipping gravelly or sandy foresets that either pass tangentially into relatively flat-lying finer-grained bottomset facies or overlie bottomsets with an angular contact. In outcrops, the foreset tops are commonly bounded by erosional surfaces and no foreset–topset transition is recognizable. Erosional surfaces are related to the formation of long-wavelength bedforms, distributary channels or delta-top incised valleys. In seismic profiles, foreset–topset transitions display rising sigmoidal, smooth-topped subhorizontal or falling stepped-topped patterns (Winsemann *et al.* 2007, 2009, 2011; Roskosch *et al.* 2015).

Topset facies associations (FA1.1). – Delta topsets are recorded mainly from GPR and seismic profiles, where these deposits form up to 10-m-thick units. They are exposed only in a few outcrops in the whole study area and comprise delta-plain deposits (FA1.1.1), long-wavelength bedforms and isolated scour fills (FA1.1.2), distributary-channel fills (FA1.1.3) and incised-valley fills (FA1.1.4).

In outcrop, the delta-plain deposits (FA1.1.1) have an overall sheet-like geometry and consist of 1–6 m thick trough cross-stratified sand, pebbly sand and gravel (facies St/Gt), which fill shallow lenticular channels (up to 10 m wide and 2 m deep) with a nested offset stacking pattern. In seismic profiles, the delta-plain deposits are characterized by horizontal high-amplitude reflectors (Winsemann *et al.* 2011). In outcrop, isolated metre-scale scours on top of truncated foresets are filled with gravelly backsets (facies Gbl).

Long-wavelength bedforms (FA1.1.2), deposited from supercritical tractional flows, consist of up to 10-m-high, slightly asymmetrical to symmetrical sediment waves with wavelengths of 60–90 m. In seismic profiles, the wave-like structures are characterized by internal convex-up parallel high-amplitude reflectors (Fig. 5A). Bedforms with shorter wavelengths of 38–45 m are associated with deep scours, filled with foresets (Fig. 5B). Based on their wavelengths and asymmetry these deposits may represent either large antidunes or net-depositional cyclic steps (Kostic 2011; Winsemann *et al.* 2011;

Muto *et al.* 2012; Cartigny *et al.* 2014). The downflow alternation with irregularly spaced scours (Fig. 5B) indicates cyclic steps or chutes-and-pools with superimposed antidunes (Postma *et al.* 2014; Zhong *et al.* 2015; Lang *et al.* 2017a). Scours are filled laterally with foresets, which more commonly occur in chutes-and-pools (Lang & Winsemann 2013; Cartigny *et al.* 2014). However, cross-strata backsets are more characteristic of cyclic-step bedforms and the latter cannot thus be ruled out. Net-erosional cyclic steps would produce trains of scours, which might have been filled subsequently by lower-energy currents during the final stage of flow. Isolated scour fills with backsets are interpreted as the preserved hydraulic jump zone of cyclic steps (Muto *et al.* 2012; Cartigny *et al.* 2014) that probably formed on the delta plain during major meltwater discharges.

Distributary-channel fills (FA1.1.3) are lens-shaped in cross-section and appear as vertically and laterally stacked lenticular deposits that are often organized into larger scale channel complexes, up to 8 m thick and ~100 m wide. Individual channels are up to 70 m wide, 1.5–5 m deep and have aspect (width/depth) ratios >14:1. In shear-wave seismic profiles, larger distributary channels are recognizable as concave-up, lenticular features with high-amplitude internal reflectors (Winsemann *et al.* 2011). At the base of these channels gravel lags are common, composed of clast-supported cobble to boulder gravel (facies B). These channel-floor deposits are overlain by trough cross-stratified cobble to pebble gravel, pebbly sand and sand (facies Gt/St). Towards the channel margins, cross-sets are finer-grained and thinner and often form climbing cosets (facies Scd). Climbing dunes formed under high suspension fall-out rates (Winsemann *et al.* 2011) and may indicate the channel-mouth zone (Ghienne *et al.* 2010; Carvalho & Vesely 2017). The upper channel fills commonly consist of fine-grained planar-parallel stratified and climbing-ripple cross-laminated fine-grained sand, silt and mud (facies Sr/FI), indicating channel abandonment (Winsemann *et al.* 2011).

Incised-valley fills (FA1.1.4) are approximately 25 m deep and 25–150 m wide, commonly flat-based and cut deeply into delta topset and foreset deposits. They form large-scale U-shaped isolated features with aspect (width/depth) ratios of 1:1 to 6:1. In seismic profiles, incised valleys are concave-up erosional features with transparent internal reflectors (Winsemann *et al.* 2011). The axial valley-fill deposits consist mainly of thick-bedded planar and trough cross-stratified sand, pebbly sand and gravel (facies St/Gp/Gt), deposited from turbulent subcritical tractional flows. Low-angle cross-stratified or sinusoidally stratified sand, pebbly sand and gravel beds (facies Sl/GI) indicate deposition from antidunes during supercritical flow conditions. As in the delta-plain distributary channels cross-sets are finer-grained and thinner towards the channel margins and often form climbing cosets (facies Scd/Sr). The internal

Table 1. Sedimentary facies of Gilbert-type delta and shoal-water delta deposits.

| Facies | Description | Interpretation |
|--------|--|--|
| B | Clast-supported cobble to boulder gravel with blocks up to 1.3 m across | Lag deposits at channel floors caused by erosion and winnowing of finer grain sizes |
| Go | Open-work gravel lenses. Lenses are commonly vertically and laterally graded with a coarse head and an upslope fining tail | Deposition by debris fall on the delta slope |
| Gmg | Massive or inversely graded matrix- or clast-supported pebble to boulder gravel. The matrix is fine- to coarse-grained sand. Long axes of large outsize clasts may be orientated parallel to dip and may show a steep upslope dipping a(p) a(i) fabric. Bed contacts are sharp and non-erosional | Deposition from non-cohesive debrisflows. The steep-clast fabric indicates laminar shear during or immediately after the flow's stop |
| Gp/Gt | Clast-supported pebble to cobble gravel with planar or trough cross-stratification. The matrix is fine- to medium-grained sand. Bed contacts are erosive | Deposits of migrating 2D and 3D dunes or transverse bars. The deposition occurred from tractional bedload flows in channels on the delta plain or sustained turbidity currents on the delta slope |
| Gl | Low-angle cross-stratified gravel. The matrix is medium- to coarse-grained sand | Deposits of breaking antidunes. Deposition from supercritical tractional flows in channels on the delta plain or supercritical turbidity currents on the delta slope |
| Gbl | Backset cross-stratified gravel that laterally may pass into low-angle cross-stratified or sinusoidally stratified sand. Backsets occur in regularly spaced scours or over the entire bed length. The gravel typically shows an upslope dipping steep-clast fabric (a(p) a(i) or b(t) b(i) fabric) | Deposits of cyclic steps. Deposition from surge-type or sustained supercritical turbidity currents on the delta slope |
| Smg | Pebbly fine- to coarse-grained massive, inversely or normally graded sand. Clasts are commonly pebble- to cobble-sized. Bed contacts are sharp or erosive | Deposition from sandy debrisflows by freezing or turbidity currents on the delta slope |
| Sbl | Backset cross-stratified pebbly sand and sand that laterally may pass into low-angle cross-stratified or sinusoidally stratified sand. Backsets occur in regularly spaced scours or over the entire bed length. Some sandy scour fills are massive, diffusely graded or deformed by dewatering structures and may pass upslope into backset cross-stratification | Deposits of cyclic steps. Deposition occurred from supercritical turbidity currents on the delta slope. Scour fills with deformed strata and dewatering structures reflect the hydraulic-jump zone of cyclic steps where rapid suspension fall-out and liquefaction of deposits occur |
| Sl | Low-angle or sinusoidally cross-stratified pebbly sand and sand. Beds may fine or coarse upwards and have internal truncation surfaces. At the base small scours filled with pebbles may occur. Upsetion the thickness of bedsets commonly increases and sigmoidal bedforms are preserved. Bed contacts are sharp or gradational | Deposits of breaking and stationary antidunes. Deposition from supercritical tractional bedload flows in channels on the delta plain or supercritical turbidity currents on the delta slope |
| Ssi | Sigmoidally cross-stratified sand and pebbly sand with well-developed topset, foreset and bottomset geometries. Bed contacts are sharp or erosive | Deposits of migrating humpback dunes. Deposition from transcritical turbidity currents on the delta slope |
| Sp/St | Fine- to coarse-grained sand and pebbly sand with planar or trough cross-stratification. Beds partly form climbing bedsets. Bed contacts are sharp or erosive | Deposits of 2D and 3D dunes or transverse bars. Deposition occurred from subcritical tractional bedload flows in channels on the delta plain or sustained turbidity currents on the delta slope |
| Scd | Planar, trough or sigmoidally cross-stratified pebbly sand and sand forming climbing bedsets. Foreset beds are partly oversteepened and contorted and may pass updip into low-angle cross-stratified sand (Sl). Bed contacts are erosive to gradational | Deposits of migrating 2D and 3D dunes or humpback dunes. Deposition from subcritical to transcritical tractional flows in channels on the delta plain or subcritical to transcritical turbidity currents on the delta slope. Climbing bedforms indicate high suspension fall-out rates, partly under hydraulic-jump conditions |
| Sr | Fine- to coarse-grained (climbing) ripple cross-laminated sand. Beds are planar or trough cross-laminated and commonly show a fining-upward where a lamination with eroded ripple stoss sides passes upwards into lamination with preserved stoss sides and into draping lamination. Bed contacts are sharp, erosive or gradational | Deposits of 2D and 3D ripples. Deposition from subcritical tractional flows in channels or interchannel areas on the delta plain or sustained subcritical turbidity currents on the delta slope and prodelta. Climbing bedforms indicate high suspension fall-out rates |
| Fl | Normally graded or massive sand that fines upwards into planar-parallel laminated and ripple-cross laminated medium- to fine-grained sand and silt, planar-parallel laminated or massive silt, mud or clay. Beds are most commonly 'incomplete' and contain both 'top-absent' or 'base-absent' successions. Bed contacts are sharp or erosive | Deposition from subcritical tractional flows or suspension fall-out on the delta plain or from waning surge-like subcritical turbidity currents on the delta slope or prodelta |

Table 2. Facies associations of (A) Gilbert-type delta and (B) shoal-water delta deposits.

| | Interpretation |
|---|--|
| Delta topsets | |
| Delta-plain deposits (FA1.1.1) Trough cross-stratified sand, pebbly sand and gravel (facies St, Gt). Troughs are 0.3–1.5 m wide, 0.15–0.5 m thick and fill shallow lenticular channels | Deposition by migrating 3D dunes in a lower flow regime of uni-directional currents (Harms <i>et al.</i> 1975; Ghienne <i>et al.</i> 2010; Winsemann <i>et al.</i> 2011) |
| Long-wavelength bedforms (FA1.1.2) Long-wavelength bedforms consist of up to 10 m high, slightly asymmetrical to symmetrical sediment waves with wavelengths of 60–90 m. The asymmetric bedforms have slightly steeper upflow (stoss) slopes than the downflow (lee) slopes and pass downflow into symmetrical bedforms. Bedforms with shorter wavelength of 38–45 m are associated with 12–40 m wide and 2–3 m deep scours, filled with foresets. These scours have an irregular spacing of 70–170 m. In outcrop, isolated scours on top of truncated foresets are about 2 m wide, 0.5 m deep and filled with gravelly backsets (facies Gbl) | Formation by large antidunes, chutes-and-pools or net-depositional cyclic steps in upper flow regime uni-directional currents (Winsemann <i>et al.</i> 2011; Muto <i>et al.</i> 2012; Cartigny <i>et al.</i> 2014; Postma <i>et al.</i> 2014; Lang <i>et al.</i> 2017a) |
| Distributary channel fills (FA1.1.3) Basal gravel lags are composed of clast-supported boulder to cobble gravel (facies B). These lag deposits are overlain by trough cross-stratified cobble to pebble gravel, pebbly sand and sand (facies Gt, St). Trough cross-strata sets are 0.2–1 m thick and troughs are 0.5–1.5 m wide. Towards the channel margins, cross-sets are finer-grained and thinner and often form climbing cosets (facies Scd). The upper channel fills commonly consist of fine-grained planar-parallel stratified and climbing-ripple cross-laminated fine-grained sand, silt and mud (facies Sr/Fl) | Deposition by migrating 3D dunes in lower flow regime uni-directional currents (Harms <i>et al.</i> 1975; Ghienne <i>et al.</i> 2010). Gravel lags indicate channel-floor deposits. Climbing dunes formed under high suspension fall-out rates (Winsemann <i>et al.</i> 2011) |
| Incised-valley fills (FA1.1.4) The axial valley-fill deposits consist mainly of thick-bedded (1–2 m) planar and trough cross-stratified sand, pebbly sand and gravel (facies St, Gp, Gt). Troughs are up 1 m deep and 3 wide. Low-angle cross-stratification or sinusoidal stratification occasionally occurs in sand, pebbly sand and gravel (facies Sl, Gl). The axial valley fills are commonly amalgamated and often show a fining-upwards-trend with a basal gravel lag (facies B), a succession of cross-stratified gravel and pebbly sand (facies St, Gp, Gt), overlain by ripple cross-laminated sand (Sr) passing upwards into draping lamination and thinly interlayered silt and mud (facies Fl). Cross-sets are finer-grained and thinner towards the valley margins and often form climbing cosets (facies Scd, Sr) | Deposition by migrating 3D dunes in lower flow regime uni-directional currents (Harms <i>et al.</i> 1975; Ghienne <i>et al.</i> 2010) and by antidunes during supercritical flow conditions (Fielding 2006). Thick planar cross-stratified gravel beds resulted from the migration of gravel bars (Massari & Parea 1990; Browne & Naish 2003). Climbing dunes at the valley margins indicate lower flow velocities and high suspension fall-out rates (Winsemann <i>et al.</i> 2011) |
| Delta foresets | |
| Foreset-bed packages I (FA1.2.1) Massive or inversely graded matrix- or clast-supported pebble to boulder gravel with sharp non-erosive basal contacts (facies Gmg). The matrix is medium- to coarse-grained sand. Many beds show upslope-dipping internal shear planes and an imbricated a(p) a(i) fabric. Bed thickness is 10–60 cm. Beds commonly have sharp, mostly non-erosional contacts. Erosion surfaces are commonly draped by thin- to medium-bedded (2–20 cm) normally graded sand (facies Smg, Fl) or low-angle cross-stratified pebbly sand beds (facies Sl) that laterally grade into fine-grained bottomset beds | Deposition from cohesionless debrisflows (Nemec 1990; Sohn <i>et al.</i> 1997). The thin sand or pebbly sand beds that drape major erosional surfaces indicate deposition from subcritical and supercritical turbidity currents (Kostic <i>et al.</i> 2002; Winsemann <i>et al.</i> 2011) |
| Foreset-bed packages II (FA1.2.2) Medium- to thick-bedded (10–60 cm) massive, normally or inversely graded matrix- or clast-supported pebble to boulder gravel (facies Gmg) and pebbly sand (facies Smg). The sorting is generally poor and the matrix consists of medium- to coarse-grained sand. Long axes of outsized clasts are often aligned parallel to the dip of bedding planes. Beds contacts are sharp, uneven and mostly non-erosional. Some pebbly sand and gravel beds are low-angle cross-stratified (facies Gl, Sl), 10–20 cm thick, and show erosional basal contacts. Occasionally isolated scours, 0.1–0.3 m deep and 0.5–1 m wide, filled with sandy or gravelly backsets occur (facies Sbl, Gbl). Clast-supported open-work boulder to pebbly gravel (facies Go) in the lower foreset or toset area are 0.6–3 m long in dip direction and 0.05–1.5 m thick. They often display a vertical normal grading and a lateral grading of a coarse head down-dip into an upslope fining tail | Deposition from non-cohesive debrisflows, sandy debrisflows (Sohn <i>et al.</i> 1997; Nemec <i>et al.</i> 1999), debris fall (Nemec 1990; Sohn <i>et al.</i> 1997; Uličný 2001) and surge-type supercritical turbidity currents (Lang <i>et al.</i> 2017b) |
| Foreset-bed packages III (FA1.2.3–FA1.2.5) FA1.2.3: Backset cross-stratified gravel and pebbly sand, alternating with low-angle cross-stratified sand and pebbly sand, climbing-ripple cross-laminated or massive sand and silt, forming small-scale (0.9–1.5 m) fining-upward successions. At the base, erosive-based gravel and pebbly sand beds frequently show backsets that fill scours with scooped basal erosion surfaces, 0.9 m to >4 m wide and 0.1–0.7 m deep (facies Gbl). The gravel commonly shows a steep upslope dipping a(p) a(i) or a(t) b(i) fabric. Some sandy scour fills are massive, diffusely graded or deformed by dewatering structures (convolute bedding and clastic dykes) and may pass upslope into backset cross-stratification. Laterally scour fills may pass into sheet-like low-angle cross-stratified or sinusoidal bedforms (facies Sbl). The overlying low-angle cross-stratified sand beds | Tractional deposition from waning, surge-type supercritical to subcritical turbidity currents that produce small-scale fining-upward successions (Postma <i>et al.</i> 2014; Ventra <i>et al.</i> 2015; Lang <i>et al.</i> 2017a, b) |

(continued)

Table 2. (continued)

| | Interpretation |
|--|---|
| <p>are 5–15 cm thick, have erosive bases and may be draped by thin (0.5–1 cm) massive silty fine-grained sand layers. They have internal truncation surfaces and may show small concave-up scours (5–10 cm wide and 2–3 cm deep) at the base filled with pebbles (facies S1). Upsection the thickness of bedsets commonly increases and sigmoidal bedforms are preserved. Occasionally gravelly or sandy sigmoidally cross-stratified deposits occur (facies Ssi). The uppermost portion of the fining-upward successions may consist of thin beds (1–10 cm thick) with climbing ripple cross-laminated silty sand or massive silt and mud (facies F1). The small-scale fining-upward sequences may be organized into larger-scale (2–3 m) coarsening or fining-upward cycles, characterized by the thickness and abundance of gravel beds</p> | |
| <p>FA1.2.4: Backset cross-stratified sand and pebbly sand, alternating with low-angle cross-stratified, sigmoidally cross-stratified and planar and trough cross-stratified sand and pebbly sand. Pebbly sand beds frequently show backsets that fill scours with concave-up geometries, 0.6–6 m long and 0.06–0.7 m deep (facies Sbl). Individual beds are 0.2–1.6 m thick, commonly fine upwards and occur over the entire foreset length. Laterally and vertically backset beds may pass into sheet-like low-angle cross-stratified (facies S1) or sinusoidal bedforms (facies Ssi), 0.2–0.7 m thick, forming dm-scale fining-upward successions. Perpendicular and oblique to flow these deposits appear as shallow troughs, filled with concentric to low-angle cross-stratified pebbly sand and sand. Finer-grained sandy beds commonly display dune-scale planar and trough cross-stratification (facies Sp, St). On average beds are 0.1–0.7 m thick. Bed contacts are sharp erosional. In the delta-toe zone well-preserved deposits of sigmoidal humpback dunes are often developed, which show typical tripartite geometries with topsets, foresets and bottomsets (facies Ssi)</p> | <p>Tractional deposition from sustained supercritical to subcritical turbidity currents (Postma <i>et al.</i> 2014; Lang <i>et al.</i> 2017a, b). The formation of sigmoidal humpback dunes requires highly aggradational conditions (Fielding 2006; Lang & Winsemann 2013; Cartigny <i>et al.</i> 2014), which prevail in the delta-foot zone</p> |
| <p>FA1.2.5: Climbing-ripple cross-laminated sand with intercalations of lenticular massive or backset cross-stratified pebbly sand and sand beds. Beds mainly consist of medium- to very thick-bedded (0.1–1.8 m) fine- to medium-grained climbing-ripple cross-laminated sand (facies Sr). Some beds contain scattered pebbles. Beds often show a fining-upward where a lamination with eroded ripple stoss sides passes upwards into lamination with preserved stoss sides and into draping lamination and very thin-bedded mud and clay beds. Ripples either migrate down-slope or upslope. More rarely, thin- to medium-bedded sand, silt and mud alternations with Bouma Ta-d divisions (facies F1), large-scale cross-stratified pebbly sand beds (facies Sp, St) or lenticular intercalations, 1.2–10 m wide and 0.2–0.8 m thick, occur that consist of massive, diffusely graded, deformed or backset cross-stratified pebbly sand and sand beds (facies Sbl)</p> | <p>Deposition by sustained subcritical turbidity flows, which produce beds without significant vertical variation in grain size (Kneller & Branney 1995; Winsemann <i>et al.</i> 2007). During higher flow conditions dune-scale cross-stratification and cyclic steps with backset cross-stratification accumulated on the lower delta slope (Postma <i>et al.</i> 2014; Lang <i>et al.</i> 2017b). Upslope migrating ripples may indicate the zone of flow transition of jets emerging from delta-plain channels (Jopling 1965)</p> |
| <p>Chute fills: In foreset packages III (FA1.2.3 and FA1.2.4) lenticular chute fills are common. The fill consists of trough cross-stratified gravel (facies Gt), overlain by massive to diffusely stratified sand (facies Smg/S1) or cross-stratified and/or ripple cross-laminated sand (facies Sp/St/Sr). Troughs of the gravelly bedforms are 1–4 m wide and 0.2–2.5 m deep and may contain cobble-sized intraclasts. Grain size and matrix content vary between individual troughs. Some coarser-grained trough fills display open framework. Occasionally found are gravelly scour fills with backset cross-stratification (facies Gbl). The laterally more persistent fine- to coarse-grained sand beds are 0.4–0.7 m thick and fine upwards. At the base of the chutes often a boulder to cobble gravel lag (facies B) occurs. Towards the top and channel margin the thickness of cross-sets commonly decreases (0.2–0.6 m) and climbing cosets are often developed. Foreset beds of the climbing (humpback) dunes (facies Scd) are partly oversteepened and contorted and pass updip into low-angle cross-stratified sand (facies S1)</p> | <p>Tractional deposition from supercritical and subcritical turbidity currents (Mulder & Alexander 2001; Winsemann <i>et al.</i> 2009). High sedimentation rates under hydraulic-jump conditions are indicated by the formation of climbing humpback dunes with oversteepened and contorted foresets (Winsemann <i>et al.</i> 2011; Lang & Winsemann 2013). The oversteepened and contorted dune foreset beds indicate liquefaction-induced slope collapse processes caused by rapid loading (Owen 1996)</p> |
| <p>Delta bottomsets</p> | |
| <p>FA1.3.1</p> | |
| <p>Low-angle cross-stratified medium- to coarse-grained sand and pebbly sand (facies S1), interbedded with massive or inversely graded pebble to cobble gravel with non-erosive bases (facies Gmg). Bed thickness ranges between 0.1 and 0.3 m. Isolated larger clasts or small gravel clusters occur in distinct sand and pebbly beds. The long axes are commonly orientated parallel to the dip of bedding planes. The low-angle cross-stratified pebbly sand and sand beds may pass downflow into climbing-dune cross-stratification (facies Scd), forming 0.2–0.3 m thick cosets. Occasionally small isolated scours occur (0.5–1 m long and 0.1–0.15 m deep) that are filled with sandy backsets or foresets (facies Sbl). In finer-grained, more sand-rich bottomset deposits low-angle and sigmoidally cross-stratified sand and pebbly sand (facies S1 and Ssi) may alternate with thin- to medium bedded (0.1–0.3 m) climbing-ripple cross-laminated sand and silt (facies Sr)</p> | <p>Deposition from cohesionless debrisflows, debris fall and supercritical to subcritical turbidity currents, partly triggered by the release of limited sediment volumes by discrete failures of upper delta-slope deposits (Nemec 1990; Sohn <i>et al.</i> 1997; Nemec <i>et al.</i> 1999; Winsemann <i>et al.</i> 2011; Gobo <i>et al.</i> 2014). Hydraulic-jump conditions in the prodelta zone led to the formation of isolated scours and the deposition of small-scale climbing dunes (Nemec <i>et al.</i> 1999; Winsemann <i>et al.</i> 2007, 2011)</p> |
| <p>FA1.3.2</p> | |
| <p>Thin- to thick-bedded (0.1–0.5 m) climbing humpback-dune assemblages (facies Scd) passing downflow into thin- to medium-bedded (0.05–0.3 m) climbing-ripple trough cross-laminated fine- to coarse-grained sand (facies Sr) and into very thin- to thin-bedded (2–10 cm) alternations</p> | <p>Deposition by turbidity currents under hydraulic-jump conditions during flow expansion at the mouth of a channel or slope break (Nemec <i>et al.</i> 1999; Macdonald <i>et al.</i></p> |

(continued)

Table 2. (continued)

| | Interpretation |
|--|--|
| of massive or planar parallel-laminated clay and planar-parallel or climbing-ripple cross-laminated silt and fine- to medium-grained sand (facies Fl). Cm-scale convolute bedding, ball and pillow structures, and flame structures are common. Bed contacts are erosional to gradational | 2009; Winsemann <i>et al.</i> 2011). The lateral facies transition from climbing dunes into finer-grained facies Sr and Fl records waning flow conditions and deposition from diluted turbidity currents |
| FA1.3.3 Thin- to medium-bedded (0.05–0.3 m) fine- to coarse-grained climbing-ripple cross-laminated sand (facies Sr). Some beds show a thin basal unit with planar-parallel lamination. Ripples are planar or trough cross-laminated and beds may show a fining-upward where lamination with eroded ripple stoss sides passes upwards into lamination with preserved stoss sides and into draping lamination. These beds may be intercalated with normally graded or massive sand that fines upwards into planar-parallel laminated and ripple cross-laminated medium- to fine-grained sand and silt, laminated silt, and finally into laminated or massive mud or clay (facies Fl) | Deposition from subcritical surge-type and sustained turbidity currents (Ashley <i>et al.</i> 1991; Kneller & Branney 1995; Mulder & Alexander 2001) |
| FA2.1 Vertically stacked sets of flat-based, convex-up, planar to sigmoidally cross-stratified medium- to coarse-grained sand and pebbly sand (facies Sp). The overall grain size of the foresets decreases upwards. Foreset beds are commonly laterally graded and have dip angles of 5–30°. Upflow foreset beds pass into subhorizontally stratified sand. Downflow foreset beds prograde over a thin (1–2 cm) subhorizontal bottomset layer. The bedsets are 1.5–2 m thick and clinofolds are partly incised by small channels (2–3 m wide and 0.2–0.5 m deep) filled with trough cross-stratified medium-grained sand (facies St) | Bedload deposition from inertia-dominated subcritical jets (Wright 1977; Postma 1990). The overall convex-up geometries, the downstream migration and the absence of major channels point to a distal delta mouthbar environment (Fielding <i>et al.</i> 2005; Lee <i>et al.</i> 2007) |
| FA2.2 0.3–1.5 m thick trough-cross stratified cobble to pebble gravel (facies Gt), alternating with 0.1–0.7 m thick sigmoidally cross-stratified (facies Ssi), trough cross-stratified (facies St), planar cross-stratified (facies Sp), low-angle cross-stratified (facies Sl) and ripple cross-laminated (facies Sr) coarse- to fine-grained sand. The ripples partly form climbing bedsets. Larger-scale convex-up sigmoidally cross-stratified sandy bedforms, 1–2 m high, may pass downflow into climbing-ripple cross-laminated sand and onlap and drape coarser-grained convex-up bedforms, partly showing upstream accretion. These deposits are arranged into metre-scale (1.5–2.5 m) fining-upward or coarsening-upward successions, bounded by major subhorizontal or slightly concave-up erosional surfaces. The bounding surfaces may be draped by thin layers of silty sand and partly show steep-flanked V-shaped scours (up to 0.5 m deep) at the base that are laterally filled with gravel. The overlying deposits may include large sandy intraclasts, up to 0.7 m in diameter. Flow directions are highly variable and show a dispersion of up to 90° | Bedload deposition from inertia-dominated supercritical to subcritical jets (Wright 1977; Postma 1990). The formation of V-shaped scours and intraclasts may be related to the formation of cyclic steps during supercritical flow conditions (Postma <i>et al.</i> 2014). Laterally overlapping delta lobes and a high dispersion of flow directions point to a proximal delta-front environment (Olariu & Bhattacharya 2006; Lee <i>et al.</i> 2007; Fidolini & Ghinassi 2016) |

architecture of the incised-valley fills is commonly characterized by an amalgamated vertical stacking of channel-fill deposits in the valley axis, and an onlapping, laterally offset stacking at the valley margins, along which high-angle slide scars and large slide blocks can be found (Winsemann *et al.* 2007, 2011). These intra-valley channels are ~5 to >40 m wide, ~2–10 m deep and show a fining-upwards-trend with a basal gravel lag (facies B), overlain by a succession of cross-stratified gravel and pebbly sand (facies St/Gp/Gt), ripple-cross-laminated sand (Sr) and thinly interlayered silt and mud (facies Fl). The multistorey and heterogeneous infills of these intra-valley channels indicate several phases of channel scouring and deposition, related to channel migration and/or variations in meltwater discharge (Olariu & Bhattacharya 2006; Winsemann *et al.* 2007, 2011). Towards the top of an incised-valley fill the channel-margin deposits locally pass into thinner-bedded, sheet-like deposits (facies Fl), onlapping directly the truncated foreset. These overbank deposits reflect an increased range of the lateral shifting of glacialfluvial channels with the decreasing valley accommodation.

Foreset facies association (FA1.2). – Delta foresets have thicknesses between 5 and 25 m and foreset beds are inclined between 5° and 34°. In strike sections, the foreset deposits form laterally and vertically stacked mounds, 15–360 m wide. The sedimentary facies of the delta foresets include a wide range of gravity-flow deposits that tend to form three distinct facies assemblages: (I) foreset-bed packages dominated by debrisflow deposits (FA1.2.1); (II) foreset-bed packages dominated by debrisflow and debris-fall deposits (FA1.2.2); and (III) foreset-bed packages deposited by supercritical and subcritical low- and high-density turbidity currents (FA1.2.3–FA1.2.5). These foreset-bed packages are often separated from one another by erosional surfaces that dip less steeply and differ in dip directions. Chute channels, 8–60 m wide and 1–5 m deep, are common in foreset packages II and III and are mainly filled with deposits of low- and high-density turbidity currents (Figs 6–8).

Foreset-bed packages I, dominated by debrisflow deposits (FA1.2.1), consist of massive or inversely graded, matrix- or clast-supported, pebble to boulder

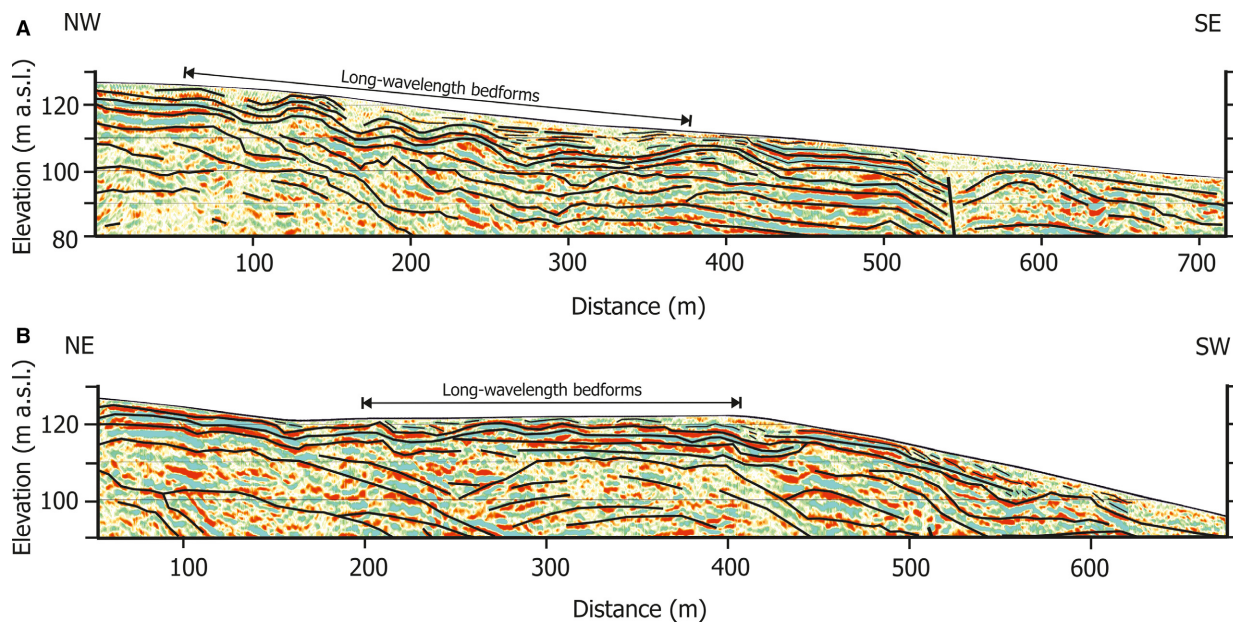


Fig. 5. Shear-wave seismic profiles of the Emme delta, showing long-wavelength bedforms that developed on the delta plain in front of an incised valley. A. Aggrading sinusoidal long-wavelength bedforms. Wavelengths range from ~60 to 90 m (FA1.1.2). B. Long-wavelength bedforms associated with irregularly spaced scours. Wavelength range from ~38 to 45 m. Scours are ~12–40 m wide, 2–3 m deep and filled with foresets (FA1.1.2). Modified from Winsemann *et al.* (2011). For this Figure we obtained permission from Wiley. [Colour figure can be viewed at www.boreas.dk]

gravel with sharp non-erosive basal contacts (facies Gmg; Fig. 6A). Many beds show upslope-dipping internal shear planes (Fig. 6B) and an imbricated a(p) a(i) fabric. In dip section these foreset beds are extensive, fairly tabular and overlie bottomset beds (FA1.3.2) with an angular contact (Fig. 6C). Internal erosion surfaces are scarce and typically have lower dip angles than the foreset bedding. Erosion surfaces are commonly draped by thin- to medium-bedded, normally graded sand (facies Smg/FI) or low-angle cross-stratified pebbly sand beds (facies SI), deposited from subcritical and supercritical turbidity currents. These beds laterally grade into fine-grained bottomset beds (facies FI, FA1.3.2). In seismic profiles, foreset-bed packages I are commonly characterized by a hummocky, transparent reflector pattern (Winsemann *et al.* 2011).

In foreset-bed packages II, dominated by debrisflow and debris-fall deposits (FA1.2.2), grain size varies from sand, pebbly sand to gravel (Fig. 6E–G) and the sorting is generally poor. The foreset facies includes massive, normally or inversely graded, matrix- or clast-supported pebble to boulder gravel (facies Gmg) and pebbly sand (facies Smg). These beds commonly have sharp, uneven and mostly non-erosional contacts, which might follow the irregular surfaces of underlying coarse gravel beds. Some pebbly sand and gravel beds are low-angle cross-stratified (facies GI/SI) and show erosional basal contacts. Occasionally found are isolated scours filled with sandy or gravelly backsets (facies Sbl/Gbl). Along dip, the beds are either laterally fairly persistent or pinching

out within a few metres. The most characteristic features of these foreset packages are clast-supported open-work gravel lenses (facies Go) in the lower foreset or toreset area (Fig. 6G). Foreset-bed packages, dominated by such gravel lenses overlie sandy bottomset beds with an angular contact, whereas the sand-richer, less steeply dipping foreset beds locally pass down-slope into sandy or gravelly bottomset deposits (Fig. 6E–H; FA1.3.1). In seismic profiles, foreset-bed packages II are characterized by mainly discontinuous low amplitude reflectors (Winsemann *et al.* 2011; Roskosch *et al.* 2015).

Foreset-bed packages III, deposited by supercritical and subcritical turbidity currents, comprise three different facies associations (FA1.2.3–FA1.2.5) that are characterized mainly by tractional bedforms. Common is a lateral fining from coarser-grained foreset-bed packages (FA1.2.3) to finer-grained foreset-bed packages (FA1.2.5). Foreset beds deposited by supercritical turbidity currents consist of laterally and vertically stacked cyclic step and antidune deposits (facies Gbl, Sbl, SI). Metre-scale fining-upward sequences and the frequent intercalation of silt and mud drapes in FA1.2.3 indicate waning, surge-type turbidity currents (Fig. 6I–M). In contrast, FA1.2.4 was deposited by more sustained supercritical to subcritical turbidity currents, indicated by thick backsets and dune-scale foresets that occur over the entire delta foreset length. Finer-grained silt or mud drapes are absent in this facies association (Fig. 7C–F). In GPR profiles backsets are characterized by lenticular elements, which are characterized by

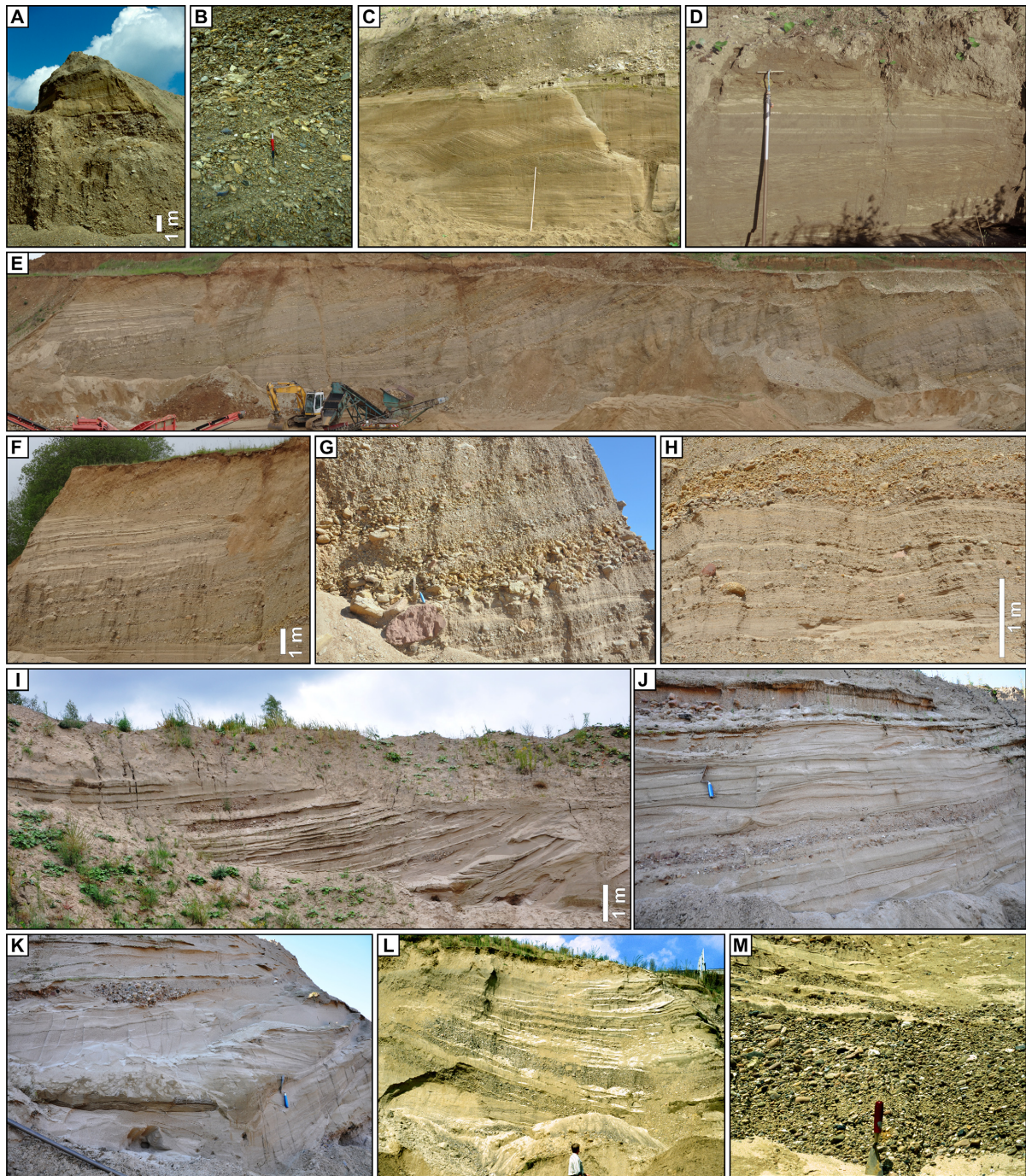


Fig. 6. Photographs of Gilbert-type delta facies associations. **A.** Foreset beds, deposited from cohesionless debrisflows (FA1.2.1). The foreset is overlain by sandy deposits of a distributary channel (FA1.1.3). **B.** Close-up view of (A) showing the steep-clast fabric of foreset beds that resulted from laminar shear. **C.** Sandy bottomset deposits with climbing humpback dune cross-stratification (FA1.3.2). The climbing humpback dunes pass laterally into climbing-ripple trough cross-laminated sand and into (D) thin-bedded alternations of clay, silt and sand (FA1.3.3). **E.** Foreset and bottomset beds, deposited from cohesionless debrisflows, debris fall and turbidity currents (FA1.2.2 and FA1.3.1). **F.** Close-up view of (E) showing sand-rich foreset beds, deposited from supercritical turbidity currents (FA1.5.3). **G.** Close-up view of (E) showing debris-fall lenses on the lower delta slope. **H.** Close-up view of (E), showing coarse-grained poorly sorted bottomset deposits, deposited from turbidity currents, diluted sandy debrisflows and debris fall (FA1.3.1). **I.** Sandy foreset beds with low-angle sinusoidal stratification, alternating with backset cross-stratified sand, pebbly sand and gravel (FA1.2.3). **J.** Close-up view of (I) showing low-angle sinusoidal stratification. These antidune deposits commonly have thin mud drapes. **K.** Close-up view of (I) showing isolated scour fills with backset cross-stratified gravel and sand. The lower scour fill shows deformed strata and dewatering structures, characteristic for the hydraulic-jump zone of cyclic steps. Laterally this scour fill passes into backset cross-stratification and more sheet-like antidune deposits. **L.** Gravelly foreset beds with backset cross-stratified gravel, alternating with low-angle sinusoidally stratified sand and pebbly sand (FA1.2.3). The deposits are organized into an overall fining-upward succession. **M.** Close-up view of (L) showing steep-clast fabric of backset cross-stratified gravel beds, interpreted as deposits of cyclic steps. [Colour figure can be viewed at www.boreas.dk]

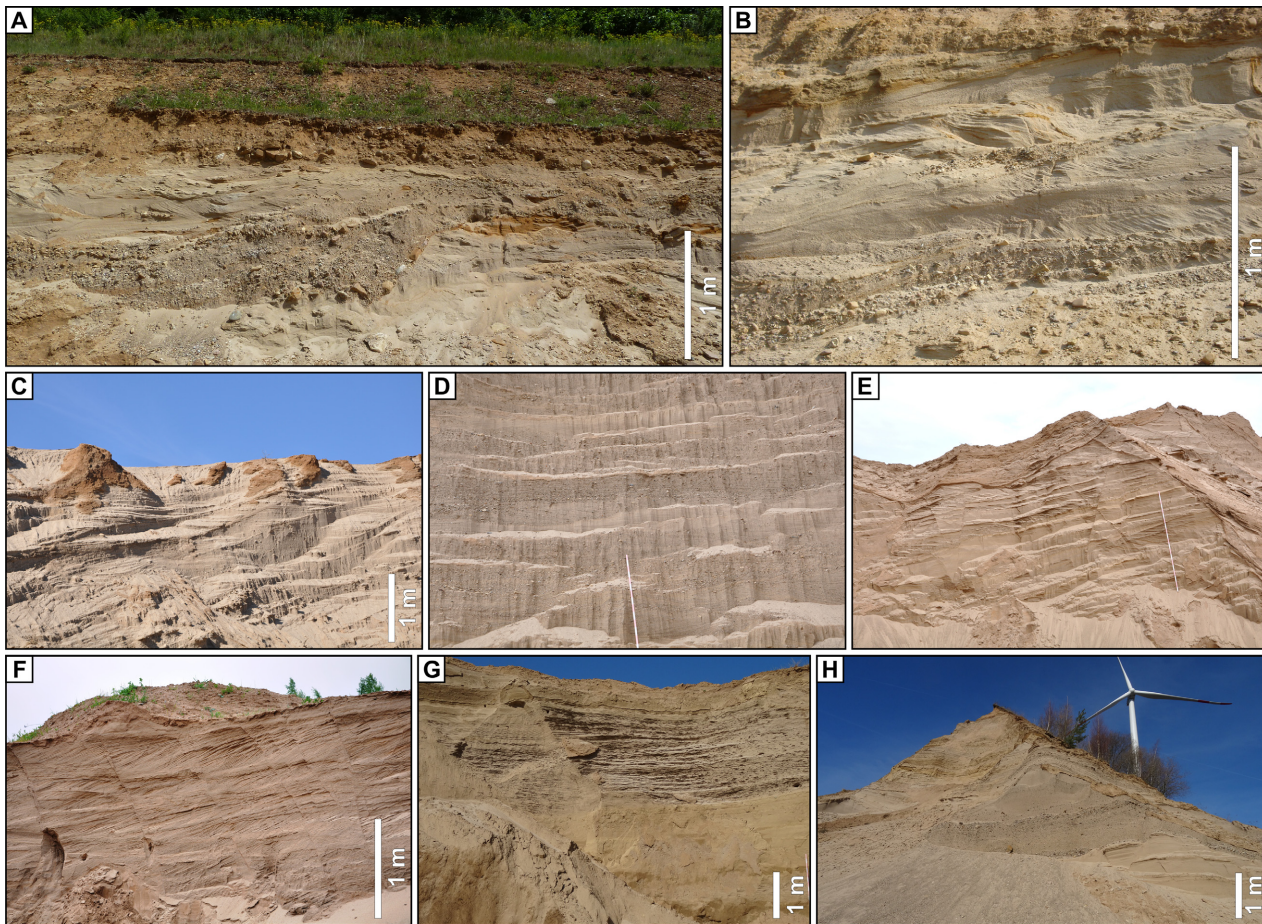


Fig. 7. Photographs of Gilbert-type delta facies associations. A. Delta-slope chute fill with coarse-grained cross-stratified gravel, overlain by climbing-dune cross-stratified sand. Note gravel lag at the base (FA1.2.3). B. Close-up view of (A) showing channel-margin deposits with climbing-dune cross-stratification. C. Foreset beds with backset cross-stratification, deposited from upslope migrating cyclic steps. The backsets occur over the entire foreset length (FA1.2.4). D. Cross-section of low-angle sinusoidal and backset cross-stratified sand and pebbly sand perpendicular to flow (FA1.2.4). E. Sandy foreset beds with low-angle cross-stratification, alternating with backset-cross stratified pebbly sand beds. The backsets occur over the entire foreset length and may pass upwards into low-angle sinusoidal antidune stratification (FA1.2.4). F. Sandy foreset beds with sigmoidally cross-stratified pebbly sand and sand (FA1.2.4). G. Sandy foreset beds with climbing-ripple cross-laminated sand (FA1.2.5). H. Delta-slope chute fill with massive gravel and pebbly sand (FA1.2.4). [Colour figure can be viewed at www.boreas.dk]

sigmoidal upslope reflectors with low to medium amplitudes (Fig. 8A, B). Farther basinwards foreset-bed packages display a higher continuity, the reflector spacing decreases and scours with backsets become rare. In the delta-toe zone well-preserved deposits of sigmoidal humpback dunes are often developed (facies Ssi), indicating less powerful transcritical sustained turbidity currents and highly aggradational conditions (Fielding 2006; Lang & Winsemann 2013; Cartigny *et al.* 2014). The upward development from trough cross-stratified pebbly sand to preserved bedforms of finer-grained humpback dunes and antidunes may indicate flow thinning over aggrading beds leading to temporarily accelerating transcritical to supercritical flow conditions (Lang & Winsemann 2013; Cartigny *et al.* 2014). Facies association FA1.2.5 (Figs 7G, 8D, E) is dominated by climbing-ripple cross-laminated sand (facies Sr), deposited from sustained subcritical turbidity flows. The

frequent occurrence of upslope migrating climbing ripples may indicate the zone of flow transition of jets emerging from the delta-plain channels. This zone is characterized by flow expansion and the formation of upslope directed large vortices (cf. Jopling 1965; Clemmensen & Houmark-Nielsen 1981; Winsemann *et al.* 2007). During higher flow conditions dune-scale cross-stratification (facies Sp/St) and cyclic steps with backset cross-stratification (facies Sbl; Fig. 8D) accumulated on the lower delta slope. These coarser-grained deposits might represent major slope failure events (Talling 2014; Dietrich *et al.* 2016; Hughes Clarke 2016) or major meltwater discharge events (Ghienne *et al.* 2010; Ventra *et al.* 2015; Carvalho & Vesely 2017). Foreset-bed packages III are commonly associated with bottomset facies association FA1.3.3. In GPR profiles the sand-rich foreset packages are characterized by high-amplitude reflectors with moderate to high continuity. Coarser-

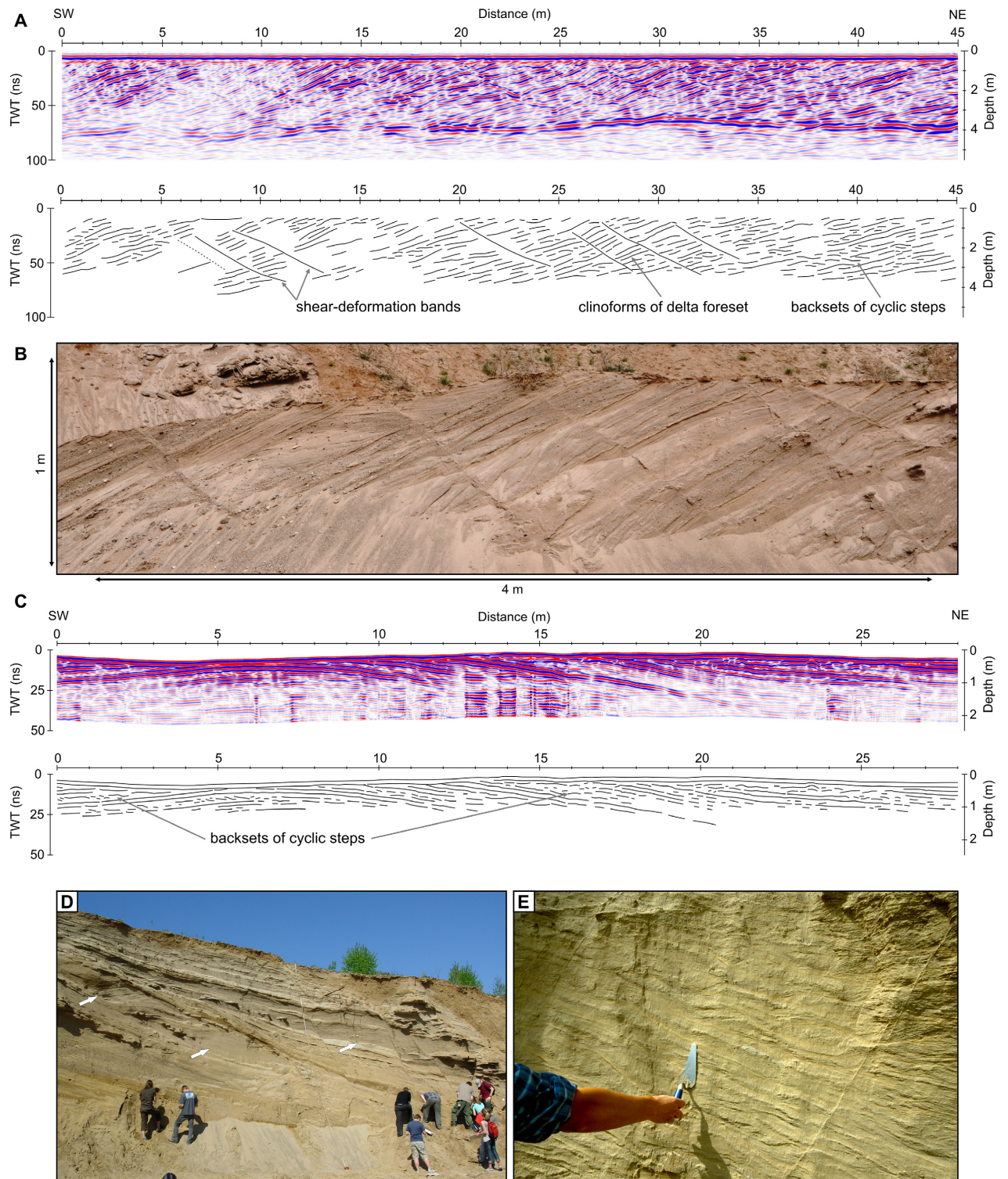


Fig. 8. GPR profiles and photographs of sandy Gilbert-type delta sediments, deposited from turbidity flows (Freden delta). **A.** GPR profile (200 MHz) of lower delta slope foreset beds (FA.1.2.4). Profile is approximately parallel to the main flow direction. The planar structural elements represent shear-deformation bands. **B.** Outcrop analogue of (A) showing lower delta slope foreset beds with backset cross-stratification and sigmoidal cross-stratification, displaced by shear-deformation bands. **C.** GPR profile (400 MHz) of fine-grained delta lobes with climbing-ripple cross-lamination. Intercalations of coarser-grained pebbly sand beds show internal backsets or dune-scale foresets (FA.1.2.5). Profile is approximately perpendicular to the main flow direction. **D.** Outcrop analogue of (C) showing climbing-ripple cross-laminated delta foresets beds with intercalations of coarser-grained pebbly sand beds with backsets. The backsets are interpreted as deposits of cyclic steps. **E.** Outcrop analogue of (C) showing thick foreset beds with climbing-ripple cross-lamination. [Colour figure can be viewed at www.boreas.dk]

grained intercalations of pebbly sand beds with backsets appear more transparent (Fig. 8C).

Bottomset facies association (FA1.3). – Delta-bottomset beds have a subhorizontal to low-angle geometry and may pass updip into steeply inclined gravelly or sandy foreset beds. Bottomsets are 1–4 m thick. They are often covered by talus and are exposed in only a few outcrops. Three main types of bottomset-bed packages (FA1.3.1–FA1.3.3) are recognized. Bottomset-bed packages I are deposited from debrisflows, debris fall and supercritical turbidity currents (FA1.3.1; Fig. 6H). These bottomset beds consists of thin- to medium-bedded massive and inversely graded gravel (facies Gmg), alternating with low-angle and sigmoidally cross-stratified pebbly sand and sand (facies Sl, Ssi). Bottomset-bed packages II and III are deposited mainly from turbidity currents. They comprise sigmoidally cross-stratified (facies Scd) and ripple trough cross-laminated (facies Sr) sand and pebbly sand, forming climbing bedsets (FA1.3.2; Fig. 6C) and climbing-ripple cross-laminated sand (facies Sr), alternating with normally graded sand to clay beds (facies Fl; FA1.3.3). In seismic and GPR profiles bottomset deposits display a parallel, continuous high-amplitude reflector pattern (Winsemann *et al.* 2011).

Shoal-water deltas (FA2)

Shoal-water deltas are characterized by 1–3 m thick gravelly or sandy delta lobes with mound-shaped geometries perpendicular to flow (Figs 9, 10). Small thickness and low angle of foresets packages reflect deposition under shallow water conditions (Postma 1990; Chough & Hwang 1997; Uličný 2001; Sohn & Son 2004; Ilgar & Nemeč 2005; Olariu & Bhattacharya 2006; Lee *et al.* 2007; Fabbriatore *et al.* 2014) where high-energy tractional flows deposited coarse-grained delta lobes. Two facies assemblages can be distinguished that differ in dip angle and sedimentary facies: (I) laterally extensive, convex-up planar to sigmoidally cross-stratified pebbly sand inclined at 5–30° (FA2.1), and (II) coarse-grained poorly sorted low-angle foresets, which consist of sigmoidally, planar-parallel and trough-cross stratified gravel and sand (FA2.2).

Laterally extensive, convex-up, sigmoidally cross-stratified sand and pebbly sand (I) (facies Sp; FA2.1; Fig. 9A, B) form vertically stacked sets of large, flat-based mouthbars (FA2.1). Up-flow foreset beds pass into subhorizontally stratified sand. Downflow foreset beds prograde over a thin (1–2 cm) subhorizontal bottomset layer. Clinofolds are partly incised by small lenticular channels, filled with trough cross-stratified medium-grained sand (facies St). In GPR profiles mouthbars are characterized by basinward-dipping moderate- to high-amplitude, continuous reflectors in flow direction (Fig. 9A) and mounded bidirectionally

downlapping reflections perpendicular or oblique to flow. Mounds are more than 25 m wide and in dip direction clinofolds can be laterally traced for more than 70 m (Winsemann *et al.* 2009; Lang *et al.* 2017b). Locally, sigmoidal geometries with transitions into bottomsets and topsets occur. The foresets are bounded by high-amplitude, gently landward dipping reflectors. Locally, small troughs and truncation of foreset boundaries can be observed. Channelized features are rare. They consist of lenticular elements, 10 m wide and up to 1 m deep, infilled by nested stacks of concentric or tangential reflectors. Up to four packages of mouthbar deposits are vertically stacked.

The overall convex-up geometries, the downstream migration and the absence of major channels in facies association FA2.1 point to a distal delta mouthbar environment (Fielding *et al.* 2005; Lee *et al.* 2007; Fabbriatore *et al.* 2014). Stable terminal distributary channels allowed for the deposition of laterally persistent downstream migrating mouthbars, which were initiated by bedload sedimentation from inertia-dominated jets (Wright 1977; Postma 1990; Olariu & Bhattacharya 2006; Fidolini & Ghinassi 2016). The slightly landward dipping laterally extensive bounding surfaces of foreset-bed packages (Fig. 9A) represent the gently dipping backs of narrow elongate mouthbars (cf. Fidolini & Ghinassi 2016).

Facies association FA2.2 (II) is characterized by medium- to thick-bedded poorly sorted trough- and planar cross-stratified cobble to pebble gravel and sand (facies Gt, Ssi, St, Sp,), sigmoidally and low-angle cross-stratified sand (facies Ssi, Sl) and ripple cross-laminated sand (facies Sr). Larger-scale convex-up bar elements partly show upstream accretion. These deposits are arranged into metre-scale fining-upward or coarsening-upward successions, bounded by major subhorizontal or slightly concave-up erosional surfaces (Fig. 10A–E). The bounding surfaces may be draped by thin layers of silty sand (facies Fl) and partly show steep-flanked V-shaped scours at the base that are laterally filled with gravel. The overlying deposits may include large sandy intraclasts, up to 0.7 m in diameter (Fig. 10D, E). Flow directions are highly variable and show a dispersion of up to 90°. The overall geometry mapped from outcrops and GPR profiles perpendicular and oblique to flow is characterized by laterally and vertically stacked mounds, 6–25 m wide and 0.3–3 m thick (Fig. 9C). In flow direction deposits are characterized by gently basinward dipping clinofolds (Fig. 9D). The lower boundaries are concordant or downlapping. Internally, parallel, continuous reflectors dominate. Amplitudes are high to low. In general, smaller mounds are associated with higher amplitude reflectors. Concave-up channelized features are 3–8 m wide and 0.5–1 m deep. Internally they comprise laterally and vertically stacked lenticular elements with inclined-tangential reflectors. The mounded delta lobes are commonly top-preserved with mounded bar

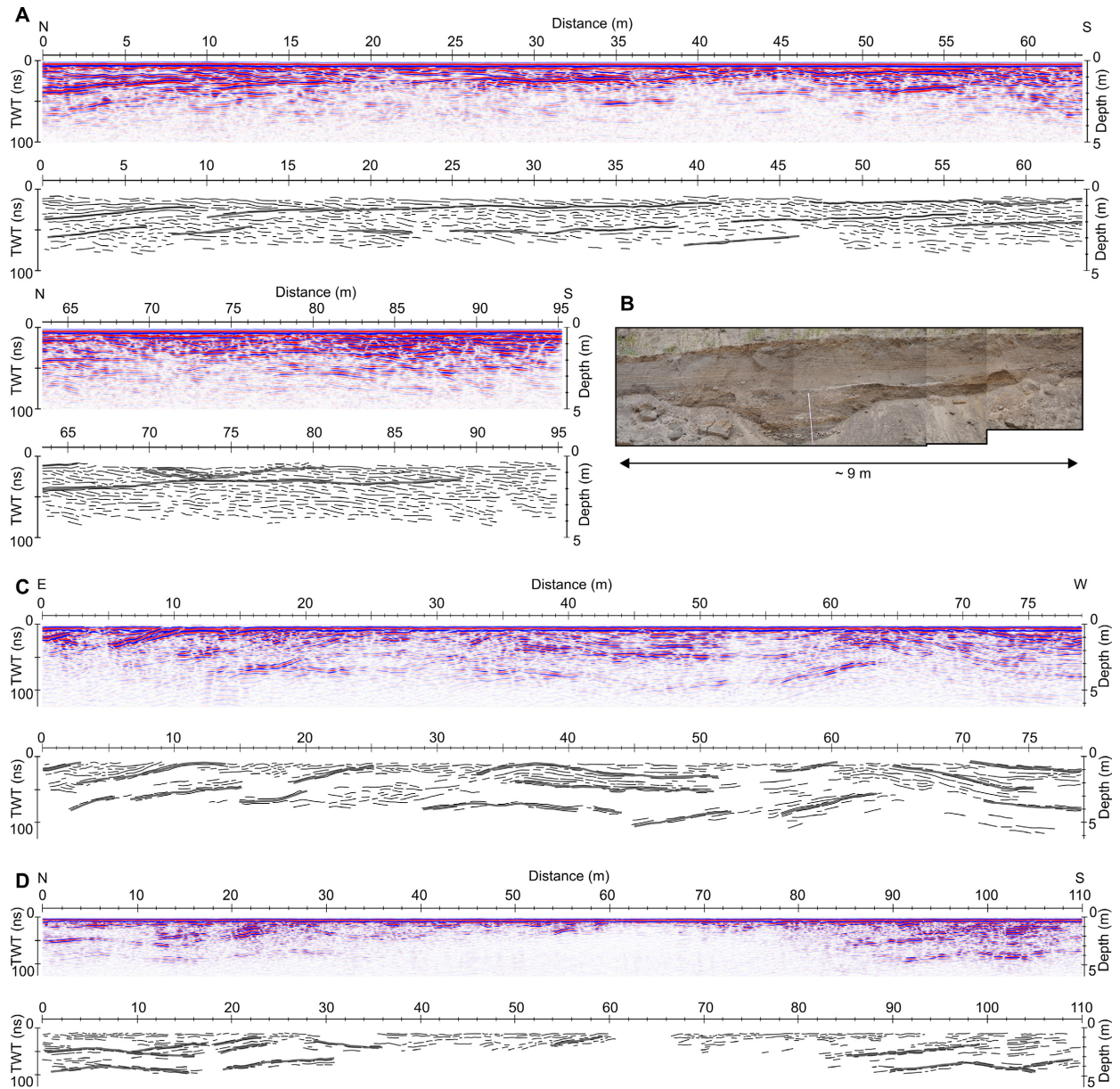


Fig. 9. GPR profiles and photopanel of shallow-water mouthbar deltas (FA2.1). **A.** GPR profile (200 MHz) of laterally persistent transgressive shoal-water mouthbar deltas. Three vertically stacked mouthbar systems are developed that are separated by landward-dipping bounding surfaces. The profile is orientated parallel to the main flow direction. **B.** Outcrop analogue of (A) showing vertically stacked, fining-upward shoal-water mouthbar deltas. **C and D.** GPR profiles (200 MHz) of forced regressive coarse-grained shoal-water mouthbar deltas. Profile C is orientated perpendicular to the main flow direction, showing laterally and vertically stacked lobes. Profile D is orientated parallel to the main flow direction, showing gently basinward dipping clinoforms. [Colour figure can be viewed at www.boreas.dk]

crests. Erosion is limited to the small-scale channel elements, which are incised into the upper parts of the delta lobes. Two to three lobe elements are vertically stacked. Compensational stacking is only observed for smaller-scale lobe elements, occurring perched in the troughs between the larger-scale elements (Fig. 9C).

Laterally overlapping coarse-grained, poorly sorted shoal-water delta lobe deposits and a high dispersion of flow directions point to frequent autocyclic lobe switching and channel avulsion in a proximal delta-front

environment (Olariu & Bhattacharya 2006; Lee *et al.* 2007; Fidolini & Ghinassi 2016). Initial mouthbars formed close to the channel axis, leading to flow splitting and the formation of new terminal distributary channels at different scales. Erosional surfaces with steep-flanked V-shaped scours and large intraclasts (Fig. 10D, E) are interpreted as bases of distributary channels (Olariu & Bhattacharya 2006; Lee *et al.* 2007). The formation of V-shaped scours and intraclasts may be related to the formation of cyclic steps during supercritical flow

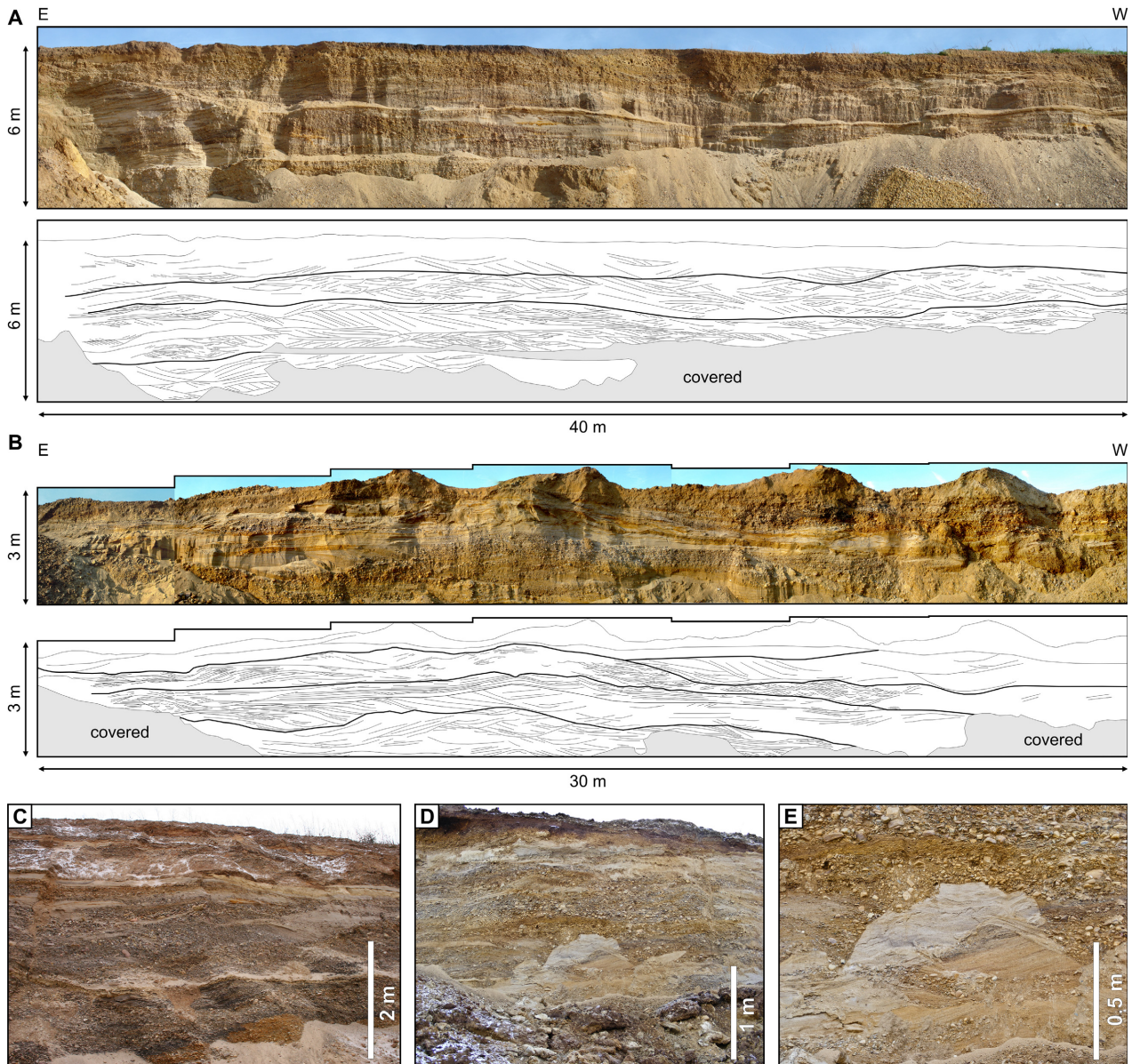


Fig. 10. Photopanel of coarse-grained forced regressive shoal-water mouthbar deposits (FA2.2), showing the sedimentary facies and major bounding surfaces. A. Sandy mouthbar deposits onlap and drape coarser-grained upstream dipping bar deposits. View is oblique to flow direction. B. The lower mouthbar deposits are overlain by coarser-grained gravel-rich more proximal mouthbar deposits. Flow is approximately perpendicular to flow. C. Close-up view of coarse-grained mouthbar deposits with trough cross-stratified gravel. D and E. Steep V-shaped scours and large intraclasts that are preserved at the base of a terminal distributary channel. [Colour figure can be viewed at www.boreas.dk]

conditions (Strong & Paola 2008; Muto *et al.* 2012; Postma *et al.* 2014). Fining-upward cycles may represent successive waning flows of major discharge events (Fielding *et al.* 2005). The slightly basinward dipping laterally extensive bounding surfaces (Fig. 9D) represent delta-lobe boundaries separating more distal from more proximal mouthbar lobes (Lee *et al.* 2007).

Deformation structures

The deformation structures within the ice-marginal deltas comprise both contractional and extensional

features. Contractional structures are generally sparse in the studied delta systems. The faults have planar to slightly listric geometries with offsets in the range of metres to tens of metres. These thrusts commonly sole out into a basal detachment, which is controlled by lithological contrasts. The most characteristic deformation structures in the studied ice-marginal deltas are normal faults and shear-deformation bands. The normal faults commonly show synsedimentary activity and two different types of fault systems can be distinguished.

The first type are normal fault systems, which are restricted to the delta body. These faults have a slightly listric

geometry and form small graben and half-graben systems (70–100 m wide), which locally show roll-over structures. Vertical offsets range between 2 and 15 m (Figs 3B, 4B). The fill of the half-grabens has a wedge-shaped geometry, with the greatest sediment thickness close to the fault, indicating synsedimentary activity. It is not clear if the faults sole out in a subhorizontal detachment (Brandes *et al.* 2011). In outcrops bed displacements along normal faults are only in the range of a few centimetres to decimetres. Some delta-slope channel fills are bounded by high-angle (65–90°) gravitational synsedimentary normal faults with vertical offsets of 0.1–1.2 m (Winsemann *et al.* 2009). Fault systems, which are restricted to the delta bodies, are related to gravitational deformation, where extension in the upper parts of the delta body is compensated by contraction at the delta-toe (Bilotti & Shaw 2005; Bini *et al.* 2007; Brandes *et al.* 2007a, 2011).

The second type are normal fault systems that originated in the underlying Mesozoic bedrock and propagated into the overlying Pleistocene delta bodies. These faults are closely spaced (10–40 m) with vertical offsets of 2–15 m and may form small-scale graben or half-graben structures (120 m wide). Wedge-shaped geometries of half-graben fills and thickening of reflector packages above the graben fills indicate synsedimentary activity (Figs 3B, 4B). Shear-deformation bands are 0–8 cm thick (mean 1.5 cm) and may displace beds by decimetres (Brandes & Tanner 2012). They form dense arrays of regularly spaced structures (Fig. 8A, B).

Fault systems that originated in the underlying Mesozoic bedrock and propagated into the overlying Pleistocene delta bodies indicate a Pleistocene reactivation of Mesozoic fault systems. This reactivation is probably related to the extension in the forebulge area of the advancing ice sheet, in combination with water and sediment loading. The dense arrays of shear-deformation bands are either related to salt movements and enhanced crestal collapse, or to reactivation of basement faults due to ice loading (Brandes & Tanner 2012; Brandes *et al.* 2018).

Discussion

The studied forced regressive ice-marginal deltas have many characteristics in common with other (glacigenic) Gilbert-type and shoal-water deltas, including the stair-stepped fan, tongue-shape or lobate geomorphology (Posamentier & Morris 2000; Ritchie *et al.* 2004a, b; Olariu & Bhattacharya 2006; Villiers *et al.* 2013), the large-scale depositional architecture (Dunne & Hempton 1984; Postma 1995; Posamentier & Morris 2000; Uličný 2001; Gutsell *et al.* 2004; Porębski & Steel 2006; Catuneanu *et al.* 2011; Eilertsen *et al.* 2011) and range of sedimentary facies (Clemmensen & Houmark-Nielsen 1981; Dunne & Hempton 1984; Nemeč 1990; Lønne 1995; Massari 1996; Sohn *et al.* 1997; Nemeč *et al.* 1999; Lønne & Nemeč 2004; Fabbriatore *et al.* 2014; Gobo

et al. 2014, 2015; Ventra *et al.* 2015; Dietrich *et al.* 2016; Carvalho & Vesely 2017; Massari 2017). Although the meltwater-source areas are likely to have yielded a significant fraction of silt and mud from glacial erosion the coarse-grained foresets are nearly devoid of silt and mud. The suspended load was probably entrained in hypopycnal plumes and was carried basinward, resulting in the deposition of thick fine-grained lake-bottom sediments (Winsemann *et al.* 2007, 2009). This sediment partitioning at the mouth of delta-feeder systems has been reported from other lacustrine and marine coarse-grained deltas (Nemeč 1990; Uličný 2001; Gobo *et al.* 2014). This corresponds with the comparatively low thickness of bottomsets, which is typical for coarse-grained bed-load dominated feeder systems, where the aggradation of the prodelta is commonly low and the delta front is characterized by a high relief (Nemeč 1990; Postma 1990; Posamentier & Morris 2000).

The frequent occurrence of bedforms deposited by supercritical turbidity flows along the foresets may be a characteristic feature of high-energy coarse-grained deltas (Massari 1996; Postma *et al.* 2014; Ventra *et al.* 2015; Dietrich *et al.* 2016; Lang *et al.* 2017b; Massari 2017). Commonly, isolated scour fills with massive, deformed or backset cross-stratified deposits were reported from the lower delta slope and delta-foot zone and related to hydraulic jumps at a break in the slope gradient, leading to rapid cut-and-fill processes (Clemmensen & Houmark-Nielsen 1981; Nemeč *et al.* 1999; Winsemann *et al.* 2007; Gobo *et al.* 2014). However, bedforms of supercritical density flows may have been overlooked in the past and interpreted as deposits of cohesionless (sandy) debrisflows or suspension-fall-out deposits from sustained turbidity flows, because only recently have numerical simulations (Kostic 2011) and flume experiments (Cartigny *et al.* 2014) allowed for a better understanding and recognition of these large-scale bedforms.

Base-level control on sedimentary facies, facies associations and stratal geometries

The sedimentary facies and facies associations defined from outcrop analysis were correlated with seismic units and subsequently assigned to base level (Fig. 11). The exposed delta sediments mainly comprise highstand, forced regressive and lowstand deposits, which record the phase of maximum lake level and subsequent lake drainage. Their features are considered as representative of delta styles in glacial lake basins, which are affected by rapid lake-level change. The good preservation of delta sediments during overall lake-level fall is related to the deglaciation stage, during which meltwater volumes, subglacial lake-outburst floods and sediment supply may increase and transfer large volume of sediments via high-magnitude discharges into deltaic environments (Evans & Clague 1994; Marren 2005; Ghienne *et al.* 2010).

Deposits of the overall transgressive phase during lake formation are mainly preserved within fine-grained lake-bottom sediments or in buried delta deposits that are recorded in seismic profiles.

Delta deposition responded to minor and major accommodation changes across shorter and longer time scales. Short-term minor variations in accommodation space were probably related to lake-level changes in the range of a few metres, caused by seasonal or decadal changes in meltwater discharge and sediment supply (cf. Lønne & Nemeč 2004; Gilbert & Crookshanks 2009). These changes mainly affected the accommodation space on the delta-brink zone, controlling the stability of the delta front and the related type of gravity-flow deposits on the delta slopes and delta bottomsets (Plink-Björklund & Steel 2004; Gobo *et al.* 2014; Talling 2014; Gobo *et al.* 2015; Dietrich *et al.* 2016; Hughes Clarke 2016). The larger-scale sediment dispersal pattern was controlled by the magnitude of major lake-level changes in the range of 20–60 m, the presence or absence of incised valleys and/or the number and depth of distributary channels and water depths (Dunne & Hempton 1984; Postma 1995; Muto & Steel 2001, 2004; Uličný 2001; Ritchie *et al.* 2004a; Olariu & Bhattacharya 2006; Winsemann *et al.* 2009, 2011; Eilertsen *et al.* 2011). The differences in sedimentary facies, thickness and slope angle of the foresets were controlled by the feeder system and accommodation available during these base-level changes (Postma 1995; Chough & Hwang 1997; Uličný 2001; Sohn & Son 2004; Winsemann *et al.* 2009, 2011; Eilertsen *et al.* 2011; Gobo *et al.* 2014, 2015).

Deposition during lake-level rise. – During overall lake-level rise an upslope shift of depocentres occurred. Vertically stacked shoal-water delta mouthbar deposits (FA2.1) formed on top of delta-plain deposits (FA1.1) during low rates of lake-level rises, when progressive aggradation of fluvial and/or delta-plain facies occurred in proximal areas (Posamentier & Morris 2000). These sandy mouthbar deposits display lake-ward dipping, laterally persistent low-angle foresets and form vertically stacked large-scale convex-up bedforms with good preservation of formsets (Fig. 9A, B), suggesting aggradation within increasing accommodation space in front of a retrograding shoal-water delta on a drowned glacial fluvial delta plain (Chough & Hwang 1997; Sohn & Son 2004; Fielding *et al.* 2005; Winsemann *et al.* 2009). In these transgressive systems the recurrence time of channel bifurcation and lobe switching of terminal distributary channels was long, allowing the channels to extend and accumulate as elongate sediment bodies (Figs 9A, B, 11; Olariu & Bhattacharya 2006). The seismic profile of the Porta fan and delta complex indicates that these shoal-water mouthbar deposits are genetically linked to high-angle Gilbert-type foresets that are exposed on the eastern margin of the truncated fan (Fig. 3A, seismic units 1–2). The sedimentary facies is

dominated by deposits of supercritical surge-type turbidity flows (FA1.2.3). The small-scale fining-upward sequences of gravelly cyclic-step deposits and sandy antidune deposits (Fig. 6I–M) were probably triggered by frequent small-volume gravitational collapses of the upper delta slope (Talling 2014; Dietrich *et al.* 2016; Hughes Clarke 2016) during high rates of delta-front aggradation (Gobo *et al.* 2014, 2015). Metre-scale fining- and coarsening-upward trends may indicate seasonal or decennial variations in meltwater flows and a related fluctuation of the lake level and the delta-plain accommodation (Gobo *et al.* 2014, 2015).

During high rates and magnitudes of lake-level rise, backstepping of delta lobes occurred, which decreased in thickness and lateral extent. The retrograding deposit profiles are stair-stepped (Fig. 3B, seismic units 1–4; Fig. 3C, seismic units 6–7), indicating a rapid upslope shift of depocentres (Muto & Steel 2001; Catuneanu *et al.* 2011; Villiers *et al.* 2013; Martini *et al.* 2017).

Deposition during highstand. – During lake-level highstand accommodation space progressively decreases and the stratal stacking pattern changes from aggradation to progradation with subhorizontal or falling delta-brink trajectories and an oblique erosional toplap geometry, which onlap the inherited depositional profile (Porębski & Steel 2006; Catuneanu *et al.* 2011). The sedimentation is characterized by thick high-angle foreset bedding, suggesting steep slopes of deep-water Gilbert-type deltas with gravity-driven flows (Nemeč 1990; Postma 1995; Uličný 2001; Eilertsen *et al.* 2011; Gobo *et al.* 2015). The highstand Gilbert-type deltas comprise both coarse-grained gravelly or finer-grained sandy systems, depending on the feeder system.

The coarse-grained gravel-rich delta systems commonly show open-work gravel lenses in the lower delta slope and toeset area (FA1.2.2), indicating frequent slope-failure events and related cohesionless debrisflow and debris fall processes (Sohn *et al.* 1997; Nemeč *et al.* 1999; Uličný 2001; Sohn & Son 2004). The alternation of steeply dipping coarse-grained foreset beds with abundant open-work gravel lenses and more gently dipping sandy foreset beds, deposited from more diluted flows (Fig. 6E–H) may point to autocyclic delta-slope steepening (Falk & Dorsey 1998; Longhitano 2008) or short variations in lake level and sediment supply, related to seasonal or decennial rates in meltwater production and sediment supply (Gilbert & Crookshanks 2009; Gobo *et al.* 2014, 2015). The debris-fall dominated foreset facies assemblage would then record deposition during times of low-magnitude lake-level rise because the aggrading delta front then tends to store sediment and undergoes frequent gravitational collapses (Gobo *et al.* 2014, 2015). The absence of major bottomset deposits during this stage is related to the predominance of low-mobility debrisflows (Nemeč 1990), whereas the turbidite-dominated facies assemblage would have formed






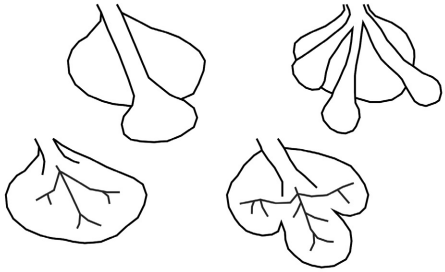
| Lake level | Depositional processes and bedforms | Stacking pattern | Geomorphology |
|---|--|--|---|
| Shoal-water deltas | | | |
| Slow lake-level rise | Tractional flows. Formation of laterally persistent mouthbars in front of stable distributary channels (FA2.1) | Vertically stacked top-preserved mouthbar deposits | Digitate, multi-tongue shaped  |
| Rapid lake-level rise | Rapid retrogradation and abandonment | | |
| Forced regression and lowstand | High-energy tractional flows. Frequent channel avulsion and lobe switching (FA2.2) | Rapid progradation with downstepping delta-brink trajectories | Lobate shape  |
| Gilbert-type deltas | | | |
| Slow lake-level rise | Delta-plain aggradation from tractional flows (FA1.1; FA2.1). Deposits of surge-type supercritical and subcritical turbidity flows on delta slopes (FA1.2.3) and in the delta-foot zone (FA1.3.3) | Rising delta-brink trajectories | Stair-stepped lobate or fan shaped, depending on the rate of lake-level rise, discharge and sediment supply  |
| Rapid lake-level rise | Not exposed | Rapid retrogradation with backstepping delta-brink trajectories. Top-preserved lobes |  |
| Lake-level highstand | Mainly by-pass on delta plain. Deposits of sustained supercritical and subcritical turbidity flows and debris fall on delta slopes (FA1.2.2; FA1.2.4; FA1.2.5). Deposits of diluted cohesionless debrisflows, debris fall, supercritical and subcritical turbidity flows in the delta-foot zone (FA1.3.1) | Progradation with subhorizontal or falling delta-brink trajectories and erosional toplap geometries | Lobate or fan shaped, depending on the discharge and sediment supply  |
| Forced regression and lake-level lowstand | Erosion and by-pass on delta plain. Partial formation of long wavelength bedforms (FA1.1.2). On the delta slope deposition by cohesionless debrisflows (FA1.2.1) or supercritical and subcritical turbidity flows (FA1.2.2; FA1.2.3; FA1.2.4). Deposition by turbidity currents under hydraulic-jump conditions in the delta-foot zone (FA1.3.1) | Rapid progradation with downstepping delta-brink trajectories and erosional toplap geometries. Either stepped-top and attached or stepped-top and detached | Stair-stepped telescoped, multi-tongue, fan shaped or lobate, depending on the rate of lake-level fall, feeder system, discharge and sediment supply  |

Fig. 11. Characteristics of deltaic deposition, stratal stacking patterns and geomorphology under lake-level change. The geomorphological sketches compile data from this study, Muto & Steel (2001, 2004), Ritchie *et al.* (2004a, b), Olariu & Bhattacharya (2006), Lee *et al.* (2007), Winsemann *et al.* (2011) and Villiers *et al.* (2013).

predominately during short periods of lake-level stillstand or slow fall, when the delta-front accommodation is at a minimum and sediment tends to be transported down-slope by erosional hyperpycnal flows (Gobo *et al.* 2014, 2015). The lateral transition into thick sandy bottomsets indicates the coeval deposition of turbidites in the delta-foot zone. Some intercalations of coarser-grained debrisflow deposits may point to deposition in front of delta-slope chutes, which transferred coarser-grained debrisflows to the delta-foot zone (Nemec 1990; Gobo *et al.* 2014).

The sand-rich highstand deltas are dominated by tractional bedforms, including climbing-ripple cross-lamination, trough cross-stratification, low-angle cross-stratification and backset cross-stratification, deposited by subcritical and supercritical turbidity currents (FA1.2.4–FA1.2.5). The grain size of the foreset-bed packages commonly decreased during progradation and a lateral facies transition from FA1.2.4 to FA1.2.5 can be observed. This might be related to an increase of the alluvial plain, increased sediment partitioning and the progressive deposition of finer-grained deposits on the delta slope (Posamentier & Morris 2000). Alternatively, the fining during progradation may be related to a decreasing water discharge and sediment supply and deposition from lower-energy density flows. Deposits of cyclic steps mainly occur within the coarsest foreset beds. In contrast to the cyclic-step deposits of the transgressive delta foresets (FA1.2.3) backsets are thicker, occur over the entire foreset length and show less variation in grain size, pointing to more sustained turbidity currents (Figs 7C–E, 8A, B). The finer-grained sandy foreset beds, deposited from migrating (humpback) dunes and ripples (Figs 7F–G, 8E) also require sustained turbidity currents that may reflect plunging hyperpycnal flows (Plink-Björklund & Steel 2004; Winsemann *et al.* 2007; Ghienne *et al.* 2010; Ventra *et al.* 2015; Carvalho & Vesely 2017) during low rates of delta-front aggradation. Gobo *et al.* (2015) suggested that a high proportion of foreset turbidites is related to a fairly persistent sediment bypass of the delta front when the delta brink-zone accommodation decreases or is at a minimum. The frequent occurrence of upslope migrating climbing ripples may indicate the zone of flow transition of plane-wall jets emerging from the delta-plain channels (cf. Jopling 1965; Clemmensen & Houmark-Nielsen 1981; Winsemann *et al.* 2007).

In contrast, Talling (2014) argued that thick tractional bedforms probably cannot be deposited by plunging hyperpycnal flows, as the suspended sediment concentrations in rivers are commonly too low, and they often do not coincide with flood peaks. However, Ghienne *et al.* (2010) were able to trace large climbing-dune cross-stratified sandstones from the delta plain into upper foreset beds, clearly pointing to the existence of plunging sediment-laden, hyperpycnal meltwater flows.

The fine-grained foresets with climbing-ripple cross-laminated sand contain a few thick intercalations of pebbly sand beds deposited from cyclic steps (Fig. 8C, D). These cyclic steps probably indicate infrequent larger slope failure events with longer run-outs, which may have been partly related to major flood peaks (Ventra *et al.* 2015). However, the exact trigger mechanism for the larger migrating supercritical bedforms remains uncertain because the foreset–topset transition zone is not preserved.

The chute fills were deposited from supercritical and subcritical turbidity currents, which may have resulted from the confinement of the currents (Gobo *et al.* 2015). High sedimentation rate under hydraulic-jump conditions are indicated by the formation of climbing humpback dunes with oversteepened and contorted foresets (Winsemann *et al.* 2011; Lang & Winsemann 2013). Synsedimentary normal faults located at the channel margins seem to have favoured a vertical channel stacking (Winsemann *et al.* 2009).

The bottomsets (FA1.3.1) of the turbidite dominated sandy foresets are only poorly exposed. GPR profiles suggest that thick bottomset deposits are absent and foreset beds downlap prodelta deposits with an angular to tangential geometry, indicating rapid progradation.

Deposition during lake-level fall (forced regression) and lake-level lowstand. – During forced regression strong progradation took place. In seismic profiles forced regressive deposits are characterized by downstepping delta-brink trajectories. The tops of forced regressive deposits are either stepped-topped and attached or stepped-topped and detached (Figs 1, 3). Fluvial incision during downstepping led to erosion of the highstand deposits and the formation of deeply incised valleys and/or distributary channels. The large scale of cross-stratification and climbing-dune assemblages in the distributary-channel and incised-valley fills suggest high-gradient streams and high flow depths (cf. Massari & Parea 1990; Breda *et al.* 2007; Winsemann *et al.* 2011). Depositional processes on the delta slopes include debrisflows, subcritical to supercritical turbidity currents or tractional currents, depending on the remaining water depth, slope steepness and type of feeder system. Therefore, the type of forced regressive and lowstand foreset packages is highly variable and may range from high-angle foreset bedding (FA1.2) to coarse-grained low-angle shoal-water mouthbar types (FA2.2) with reduced thickness (Fig. 11).

The development of stepped-topped detached Gilbert-type delta deposits was favoured by high magnitudes of lake-level fall, which promoted the development of incised valleys and the deposition of detached forced regressive coarse-grained delta lobes in front of the valleys (Winsemann *et al.* 2011), as shown in numerical simulations by Ritchie *et al.* (2004a).

Initial valley incision was probably caused by the formation of cyclic steps during rapid base-level fall (Strong & Paola 2008; Winsemann *et al.* 2011; Muto *et al.* 2012). Long-wavelength bedforms (FA1.1.2; Fig. 5) on the delta plain of the Emme delta, which formed during final lake drainage, provide evidence for incision by supercritical flows. Coeval sediments of the delta-foot zone may be represented by thick sand beds with climbing humpback-dune stratification (FA1.3.1; Fig. 6C), which record high-energy turbulent waning flows under hydraulic-jump conditions at the mouth of the incised valley channel (Winsemann *et al.* 2011). The incised valleys captured the sediment and focussed the sediment supply to coarse-grained regressive lobes in front of the incised valley, leading to the development of digitate, tongue-shaped delta morphologies. These forced regressive deposits consist of sharp-based, high-angle foreset-bed packages (30° – 10°), up to 25 m thick. The height indicates that these forced regressive deltas prograded into relatively deep water. These foreset deposits are dominated by debrisflow deposits (FA1.2.1; Fig. 6A–C) that correspond with strong fluvial erosion, a related high sediment supply to the delta front where debrisflows were deposited en masse when the slope diminished (Ilgar & Nemeč 2005; Winsemann *et al.* 2011). The coarse-grained debrisflow dominated forced regressive delta lobes may be downlapped and partly overlain by smaller-scale sandy delta lobes, deposited from debrisflows and turbidity currents (FA1.2.2) that record an upslope-shift of depocentres during valley back-filling. Valley filling mainly occurred during decreasing rates of lake-level fall and low base level (Blum & Törnqvist 2000; Winsemann *et al.* 2007, 2011; Petter & Muto 2008). The formation of attached forced regressive delta deposits was favoured by a lower rate and magnitude of lake-level fall, a high rate of sediment supply and relatively steep slope gradients (Posamentier & Morris 2000; Ritchie *et al.* 2004a, b; Catuneanu *et al.* 2011), causing only minor incision in the upper portion of the deltas. The formation of relatively fixed, deep distributary channels, incised into the older delta plain and delta foresets, hindered major lateral delta-lobe shifting and led to the formation of various delta lobes that fringe and downlap the older delta body (Winsemann *et al.* 2011). The sedimentary facies of foresets and chute fills is dominated by tractional bedforms (FA1.2.3–FA1.2.4) with a high variability in grain size, probably deposited from plunging sediment-laden, hyperpycnal meltwater flows (cf. Ghienne *et al.* 2010; Gobo *et al.* 2014, 2015).

Coarsening-upward, prograding, shoal-water delta systems are indicative of forced regressive systems (Olariu & Bhattacharya 2006; Lee *et al.* 2007) where high-energy flows entered shallow water and a strong deceleration of the flow led to rapid deposition and aggradation of the sediment in the terminal distributary channel area (Dunne & Hempton 1984; Postma 1995; Uličný 2001; Sohn & Son 2004; Ilgar & Nemeč 2005).

Some channel bases show steep-flanked V-shaped scours and large intraclasts (Fig. 10D, E). These features are common in terminal distributary channels (Olariu & Bhattacharya 2006; Lee *et al.* 2007) and might be related to the formation of cyclic steps during base-level fall or major drainage events, when supercritical flow conditions established (Strong & Paola 2008; Muto *et al.* 2012). The presence of upstream accretion suggests that these lobes were quickly abandoned (Lee *et al.* 2007). The mound-shaped geometries and large range of palaeocurrent directions suggest a series of coalescing depositional lobes, expanding into the lake basin and creating a coarse-grained lower fringe, downlapping the older steeply dipping Gilbert-type delta foresets. Compared to transgressive mouthbar systems coarse-grained forced regressive shoal-water deltas have a larger number of terminal distributary channels and much shorter recurrence intervals of channel bifurcation, avulsion and lobe switching, resulting in an overall lobate shape (Fig. 11; Olariu & Bhattacharya 2006; Lee *et al.* 2007). Coeval channel abandonment and decrease in the number of channels may occur in upper parts of the delta, leading to incision and increased discharge through the main distributary channels in the upper delta plain (Olariu & Bhattacharya 2006). In modern examples, commonly no major incision at the top of mouthbars has been observed and major incision is therefore regarded as indicative of base-level fall or major drainage events (Olariu & Bhattacharya 2006). However, the forced regressive coarse-grained mouthbar deposits of the study area are mainly vertically stacked, have partly well-preserved bar tops and are only slightly progradational (Figs 9C, D, 10). This indicates that deposition took place into relatively ‘deep’ water (several metres) that provided sufficient accommodation space and prevented strong erosion and bypass.

Deformation structures

The deformation structures within the ice-marginal deltas comprise both contractional and extensional features, which are related to (i) gravitational tectonics; (ii) glacioteconics, (iii) crestal collapse above salt domes, and (iv) postglacial faulting during glacial-isostatic adjustment (Brandes *et al.* 2011; Winsemann *et al.* 2011). A neotectonic component cannot be ruled out in some cases (Brandes & Tanner 2012).

Gravitational tectonics. – Many river deltas show gravitational deformation that is expressed in a linked extensional and compressional fault system, where extension in the upper parts of the delta body (Figs 3B, 4B) is compensated by contraction at the delta-toe (Bilotti & Shaw 2005; Bini *et al.* 2007; Brandes *et al.* 2007a, 2011). The extension in the upper part of the delta leads to the formation of basinward-dipping listric growth faults and half-graben structures. At the toe, compressional featur-

res like thrusts and folds occur (King *et al.* 2010). The normal faults and the thrusts are commonly rooted in a basal detachment that links both structural regimes (Brandes *et al.* 2007b). Such a basal detachment is often controlled by overpressured shale (Cobbold *et al.* 2004) or major lithological contrasts (Brandes *et al.* 2011). Gravitational deformation is not restricted to large deltas at continental margins with a long life span, but also occur in small lake deltas (Bini *et al.* 2007; Brandes *et al.* 2011) and can be also reproduced by metre-scale analogue models (McClay *et al.* 1998, 2003) and flume-tank experiments (Heller *et al.* 2001). In the study area, lithological contrasts between the Mesozoic bedrock and the overlying Pleistocene coarse-grained delta deposits may have supported the development of local detachments, which decoupled the gravitationally spreading delta body from the underlying bedrock. In some parts of the ice-marginal deltas fine-grained lake-bottom sediments underlie the delta and may have supported the development of a basal detachment (Brandes *et al.* 2011). The apparent absence of gravitational compression structures in the studied delta systems could be an effect of the limited upslope extension. Alternatively, these compressional structures are present but have not been recorded in the seismic profiles.

Glaciotectonic deformation. – Glaciotectonic deformation seems to play a minor role and only a few thrust sheets have been observed in sandy delta deposits. One reason might be that forced regressive delta systems commonly reflect lake drainage during an overall phase of ice retreat (Powell 1990; Ashley 1995; Lønne 1995; Winsemann *et al.* 2011; Girard *et al.* 2015). Additionally, the stable position of many deltas in front of bedrock highs prevented ice advance and related glaciotectonic deformation. However, the Elsterian Betheln delta must have been overridden by ice during the subsequent Saalian glaciation (Roskosch *et al.* 2015). A possible explanation could be an effective decoupling of the ice from the underlying sediments, which is often controlled by the water pressure at the ice/sediment interface (Kjær *et al.* 2006), where an increase in water pressure can cause localized ice/bed decoupling (Fischer *et al.* 2011). An additional controlling factor for the deformation is the rheology of the material. The lack of deformation could be caused by the presence of frozen sediment, which is more stable (cf. Tylmann *et al.* 2012) and thus potentially less prone to deformation. Another option to explain the absence of glaciotectonic deformation structures is that some of the outcrops are probably too small to show these features, especially when the structures are large and the spacing between the individual thrust planes is high.

Deformation by dead-ice melting. – Normal faults in ice-marginal deposits have often been regarded as diagnostic for the melting of dead ice in the subsurface (Selsing 1981; Prange 1995; Juschus 2001). Characteristic for dead-ice

melting is a circular pattern with strongly curved faults in the sediments, reflecting the shrinking of the buried ice block and the related collapse of the hanging-wall material. Such a circular fault pattern can be observed around actively melting dead-ice blocks (Kjær & Krüger 2001) and can be also reproduced by analogue models that simulate depletion-related surface effects (Poppe *et al.* 2015). However, our field examples clearly indicate that dead-ice melting did not play a major role in the formation of normal faults.

Crestal collapse above salt domes. – The fill of the Central European Basin System is characterized by a large number of salt structures. Many of them reach close to the earth's surface and consequently, salt movements can have an impact on the Pleistocene sediments. Lang *et al.* (2014) showed in their modelling study that salt structures can be reactivated by ice-loading. An ice advance towards a salt structure causes salt flow from the source layer below the ice sheet towards the salt structure, resulting in uplift. When the diapir is overridden by the ice sheet the salt structure is pushed down. During ice retreat large parts of the displacement are compensated by a reversal of the salt flow, resulting in a renewed uplift. In such a setting, crestal collapse with normal faulting can be a common trigger for extensional deformation (Currie 1959; Alves *et al.* 2009). Comparable phenomena were shown by Lehné & Sirocko (2005) in NW Germany and Al Hseinat *et al.* (2016) for the Baltic Sea, where faulting and surface subsidence is related to ongoing movements along local graben structures and the rise of salt diapirs.

Postglacial faulting during glacial-isostatic adjustment. – Glacial-isostatic adjustment can lead to the reactivation of pre-existing faults in the subsurface due to lithospheric stress field changes as a consequence of the growth and decay of large ice sheets (Kukkonen *et al.* 2010). Pre-existing faults in the basement can be reactivated and propagate into the overlying sediments that sealed the tip lines of the faults (Brandes *et al.* 2011). Seismic profiles of the Emme delta (Fig. 3B) and the Porta fan and delta complex (Fig. 3A) show normal fault systems developed in Mesozoic rocks, which can be traced into the overlying Pleistocene sediments. The reactivation of the Mesozoic normal faults in this location is interpreted as a consequence of extension in the forebulge area of the advancing ice sheet, in combination with loading by a glacial lake (Brandes *et al.* 2011). The fault activity ceased after the lake had considerably drained, probably indicating that fault activity in these cases was controlled by water load and water pressure and that below a critical threshold fault activity ceased (Brandes *et al.* 2011). The dense arrays of shear-deformation bands (Fig. 8A, B), which are developed within the Freden delta, also formed above the tip line of buried Mesozoic faults and therefore most likely

indicate a fault reactivation due to lithospheric stress changes caused by glacial-isostatic adjustment during MIS 8 (Brandes *et al.* 2018).

Conclusions

The studied forced regressive ice-marginal deltas are considered as representative of delta styles in glacial lake basins, affected by rapid base-level fall. They have many characteristics in common with other (glaciogenic) Gilbert-type and shoal-water mouthbar type deltas, including the stair-stepped fan, lobate or more digitate tongue-shape geomorphology, the large-scale depositional architecture and range of sedimentary facies.

The frequent occurrence of bedforms deposited by supercritical turbidity flows along the foresets may be a characteristic feature of high-energy ice-marginal deltas. Bedforms typically comprise laterally and vertically stacked successions of cyclic steps and antidunes. Trigger mechanisms of supercritical flows were hyperpycnal meltwater flows and slope-failure events in response to accommodation changes on the delta plain.

Delta deposition responded to minor and major accommodation changes across shorter and longer time scales. Short-term minor variations in accommodation space were probably related to lake-level changes in the range of a few metres, caused by seasonal or decadal changes in meltwater discharge and sediment supply. These changes mainly affected the accommodation space on the delta-brink zone, controlling the stability of the delta front and the related type of gravity flow deposits. Surge-type (supercritical) turbidity currents were probably triggered by small-volume gravitational collapses of the upper delta slope during periods of slow lake-level rise when high rates of delta-front aggradation occurred. In contrast, more sustained (supercritical) turbidity currents were probably triggered during lake-level highstand and lowstand by hyperpycnal plunging meltwater flows, when accommodation space on the delta plain was low.

The larger-scale depositional delta architecture was controlled by the magnitude and rate of major lake-level changes. The differences in sedimentary facies, thickness and slope angle of the foresets during forced regression were controlled by water depth, the presence or absence of incised valleys and/or the number and depth of distributary channels. Incised valleys formed during high-magnitude lake-level falls. These deep valleys focussed the sediment supply to coarse-grained elongate, tongue-shaped lobes, which were mainly deposited by cohesionless debrisflows. During lower magnitudes of lake-level fall or high-magnitude falls with high sediment supply attached sand-rich forced regressive aprons formed. If water depths became very low coarse-grained shoal-water mouthbar deltas formed that fringe and downlap the older Gilbert-type deltas.

The exposed delta sediments mainly comprise highstand, forced regressive and lowstand deposits, which record the phase of maximum lake level and subsequent successive lake drainage. The stair-stepped profiles of the delta systems reflect the progressive basinward lobe deposition during forced regression when the lakes successively drained. Deposits of the stair-stepped transgressive delta systems are buried and downlapped by the younger forced-regressive deposits and only deposits of the maximum lake-level highstand are preserved in geomorphology, forming the uppermost unit of the delta systems. The good preservation of delta sediments during overall lake-level fall is related to the deglaciation stage, during which meltwater volumes and sediment supply are high. Depending on the rate and magnitude of lake-level fall trumpet-shaped deeply incised valleys or a larger number of deep distributary channels formed, leading to telescoping, tongue-shaped, fan-shaped or lobate Gilbert-type delta morphologies. Forced-regressive shoal-water mouthbar deltas are typically lobate, which resulted from the coalescence of multiple terminal distributary channels and mouthbars. In contrast, shoal-water deltas deposited during transgression have more stable channels and the recurrence time for channel bifurcation and lobe switching is long, allowing the channels to extend and accumulate as elongate sediment bodies with a more digitate tongue-shape.

Deformation structures within the ice-marginal deltas comprise both contractional and extensional features, which are related to (i) gravitational delta tectonics; (ii) glaciotectonics, (iii) crestal collapse above salt domes and (iv) postglacial faulting during glacial-isostatic adjustment. In some cases, a neotectonic component cannot be ruled out. Dead-ice melting did not play a major role in the formation of normal faults.

Acknowledgements. – We thank W. Nemeč, an anonymous reviewer and editor J. A. Piotrowski for constructive comments, which helped to improve the manuscript. S. Cramm, D. Epping, S. Grüneberg, R. Meyer, W. Rode and D. Vogel (all LIAG) supported the seismic and ground-penetrating radar surveys. Borehole data were provided by LBEG (Hannover) and digital elevation models by the LGN Hannover and Bezirksregierung Köln. Fugro Consult GmbH provided GeODin software for data management. We thank A. Osman, J. Roskosch, H. Thöle, M. Wahle and A. Weitkamp for discussion and help with fieldwork. F. Busch carried out GIS work. Special thanks go to the owners of the open-pits for the permission to work on their properties. Partial funding of the research work by MWK Niedersachsen (Project 11.2-76202-17-7/08) and Leibniz Forschungsinitiative FI:GEO (Leibniz Universität Hannover) is greatly appreciated.

References

- Al Hseinat, M., Hübscher, C., Lang, J., Lüdmann, T., Ott, I. & Polom, U. 2016: Triassic to recent tectonic evolution of a crestal collapse graben above a salt-cored anticline in the Glückstadt Graben/North German Basin. *Tectonophysics* 680, 50–66.
- Alves, T., Cartwright, J. & Davies, R. 2009: Faulting of salt withdrawal basins during early halokinesis: effects on the Paleogene Rio Doce Canyon system (Espírito Santo Basin, Brazil). *AAPG Bulletin* 93, 617–652.

- Ashley, G. M. 1995: Glaciolacustrine environments. In Menzies, J. (ed.): *Modern Glacial Environments*, 417–444. Butterworth-Heinemann, Oxford.
- Ashley, G. M., Boothroyd, J. C. & Borns, H. W., Jr. 1991: Sedimentology of late Pleistocene (Laurentide) deglacial-phase deposits, eastern Maine; an example of a temperate marine grounded ice sheet margin. In Ashley, J. B. & Ashley, G. M. (eds.): *Glacial Marine Sedimentation, Paleoclimatic Significance*, 107–125. *Geological Society of America Special Paper* 261.
- Bilotti, F. & Shaw, J. H. 2005: Deep-water Niger delta fold and thrust belt modelled as a critical-taper wedge: the influence of elevated basal fluid pressure on structural styles. *AAPG Bulletin* 89, 1475–1491.
- Bini, A., Corbari, D., Falletti, P., Fassina, M., Perotti, C. R. & Piccin, A. 2007: Morphology and geological setting of Iseo Lake (Lombardy) through multibeam bathymetry and high-resolution seismic profiles. *Swiss Journal of Geosciences* 100, 23–40.
- Blum, M. D. & Törnqvist, T. E. 2000: Fluvial responses to climate and sea-level change: a review and look forward. *Sedimentology* 47, 2–48.
- Brandes, C. & Tanner, D. 2012: Three-dimensional geometry and fabric of shear deformation bands in unconsolidated Pleistocene sediments. *Tectonophysics* 518–521, 84–92.
- Brandes, C., Astorga, A., Back, S., Littke, R. & Winsemann, J. 2007a: Fault controls on sediment distribution patterns, Limón Basin, Costa Rica. *Journal of Petroleum Geology* 30, 25–40.
- Brandes, C., Astorga, A., Back, S., Littke, R. & Winsemann, J. 2007b: Deformation style and basin-fill architecture of the offshore Limón Back-arc basin (Costa Rica). *Marine and Petroleum Geology* 24, 277–287.
- Brandes, C., Igel, J., Loewer, M., Tanner, D. C., Lang, J., Müller, K. & Winsemann, J. 2018: Visualisation and analysis of shear-deformation bands in unconsolidated Pleistocene sands using ground-penetrating radar: implications for paleoseismological studies. *Sedimentary Geology* 367, 135–145.
- Brandes, C., Polom, U. & Winseman, J. 2011: Reactivation of basement faults: interplay of ice-sheet advance, glacial lake formation and sediment loading. *Basin Research* 23, 53–64.
- Breda, A., Mellere, D. & Massari, F. 2007: Facies and processes in a Gilbert-delta-filled incised valley (Pliocene of Ventemiglia, NW Italy). *Sedimentary Geology* 200, 31–55.
- Brookfield, M. W. & Martini, I. P. 1999: Facies architecture and sequence stratigraphy in glacially influenced basins: basic problems and water-level/glacier input-point controls (with an example from the Quaternary of Ontario, Canada). *Sedimentary Geology* 123, 183–197.
- Browne, G. H. & Naish, T. R. 2003: Facies development and sequence architecture of a late Quaternary fluvial-marine transition, Canterbury Plains and shelf, New Zealand: implications for forced regressive deposits. *Sedimentary Geology* 158, 57–86.
- Bullimore, S., Henriksen, S., Liestøl, F. M. & Helland-Hansen, W. 2005: Clinoform stacking patterns, shelf-edge trajectories and facies associations in Tertiary coastal deltas, offshore Norway: implications for the prediction of lithology in prograding systems. *Norwegian Journal of Geology* 85, 169–187.
- Carling, P. A. 2013: Freshwater megaflood sedimentation: what can we learn about generic processes? *Earth-Science Reviews* 125, 87–113.
- Carrivick, J. L. & Tweed, F. S. 2013: Proglacial lakes: character, behavior and geological importance. *Quaternary Science Reviews* 78, 34–52.
- Cartigny, M. J. B., Ventra, D., Postma, G. & van den Berg, J. H. 2014: Morphodynamics and sedimentary structures of bedforms under supercritical-flow conditions: new insights from flume experiments. *Sedimentology* 61, 712–748.
- Carvalho, A. H. & Vesely, F. F. 2017: Facies relationships recorded in a Late Paleozoic fluvio-deltaic system (Paraná Basin, Brazil): insights into the timing and triggers of subaqueous sediment gravity flows. *Sedimentary Geology* 352, 45–62.
- Catuneanu, O., Galloway, W. E., Kendall, C. G. S., Miall, A. D., Posamentier, H. W., Strasser, A. & Tucker, M. 2011: Sequence stratigraphy: methodology and nomenclature. *Newsletters on Stratigraphy* 44, 173–245.
- Chough, S. K. & Hwang, I. G. 1997: The Dulsung fan delta, SE Korea: growth of delta lobes on a Gilbert-type topset in response to relative sea-level rise. *Journal of Sedimentary Research* 67, 725–739.
- Clemmensen, L. B. & Houmark-Nielsen, M. 1981: Sedimentary features of a Weichselian glaciolacustrine delta. *Boreas* 10, 229–245.
- Cobbold, P. R., Mourgues, R. & Boyd, K. 2004: Mechanism of thin-skinned detachment in the Amazon Fan: assessing the importance of fluid overpressure and hydrocarbon generation. *Marine and Petroleum Geology* 21, 1013–1025.
- Currie, J. B. 1959: Role of concurrent deposition and deformation of sediments in development of salt-dome graben structures. *AAPG Bulletin* 40, 1–16.
- Dietrich, P., Ghienne, J.-F., Normandeau, A. & Lajeunesse, P. 2016: Upslope-migrating bedforms in a proglacial sandur delta: cyclic steps from river-derived underflows? *Journal of Sedimentary Research* 86, 113–123.
- Dietrich, P., Ghienne, J. F., Schuster, M., Lajeunesse, P., Nutz, A., Deschamps, R., Roquin, C. & Düringer, P. 2017: From outwash to coastal systems in the Portneuf-Forestville deltaic complex (Québec North Shore): anatomy of a forced regressive deglacial sequence. *Sedimentology* 64, 1044–1078.
- Dunne, L. A. & Hempton, M. R. 1984: Deltaic sedimentation in the Lake Hazar pull-apart basin, south-eastern Turkey. *Sedimentology* 31, 401–412.
- Eilertsen, R. S., Corner, G. D., Aasheim, O. & Hansen, L. 2011: Facies characteristics and architecture related to palaeodepth of Holocene fjord-delta sediments. *Sedimentology* 58, 1784–1809.
- Eissmann, L. 2002: Quaternary geology of eastern Germany (Saxony, Saxony-Anhalt, South Brandenburg, Thüringia), type area of Elsterian and Saalian Stages in Europe. *Quaternary Science Reviews* 21, 1275–1346.
- Evans, S. G. & Clague, J. J. 1994: Recent climatic change and catastrophic geomorphic processes in mountain environments. *Geomorphology* 10, 107–128.
- Fabbricatore, D., Robustelli, G. & Muto, F. 2014: Facies analysis and depositional architecture of shelf-type deltas in the Crati Basin (Calabrian Arc, south Italy). *Italian Journal of Geosciences* 133, 131–148.
- Falk, P. D. & Dorsey, R. J. 1998: Rapid development of gravelly high-density turbidity currents in marine Gilbert-type fan deltas, Loreto Basin, Baja California Sur, Mexico. *Sedimentology* 45, 331–349.
- Fidolini, F. & Ghinassi, M. 2016: Friction- and inertia-dominated effluents in a lacustrine, river-dominated deltaic succession (Pliocene Upper Valdarno Basin, Italy). *Journal of Sedimentary Research* 86, 1083–1101.
- Fielding, C. R. 2006: Upper flow regime sheets, lenses and scour fills: extending the range of architectural elements for fluvial sediment bodies. *Sedimentary Geology* 190, 227–240.
- Fielding, C. R., Trueman, J. D. & Alexander, J. 2005: Sharp-based, flood-dominated mouth bar sands from the Burdekin river delta of northeastern Australia: extending the spectrum of mouth-bar facies, geometry, and stacking patterns. *Journal of Sedimentary Research* 75, 55–66.
- Fischer, U. H., Mair, D., Kavanaugh, J. L., Willis, I., Nienow, P. & Hubbard, B. 2011: Modelling ice-bed coupling during a glacier speed-up event: Haut Glacier d' Arolla, Switzerland. *Hydrological Processes* 25, 1361–1372.
- Ghienne, J.-F., Girard, F., Moreau, J. & Rubino, J.-L. 2010: Late Ordovician climbing dune assemblages: a signature of outburst flood in proglacial outwash environments? *Sedimentology* 57, 1175–1198.
- Gilbert, R. & Crookshanks, S. 2009: Sediment waves in a modern high-energy glaciolacustrine environment. *Sedimentology* 56, 645–659.
- Gilbert, G. L., Cable, S., Thiel, C., Christiansen, H. H. & Elberling, B. 2017: Cryostratigraphy, sedimentology, and the late Quaternary evolution of the Zackenberg River delta, northeast Greenland. *The Cryosphere* 11, 1265–1282.
- Girard, F., Ghienne, J. F., Du-Bernard, X. & Rubino, J. L. 2015: Sedimentary imprints of former ice-sheet margins: insights from an end-Ordovician archive (SW Libya). *Earth-Science Reviews* 148, 259–289.
- Girard, F., Ghienne, J. F. & Rubino, J. 2012: Occurrence of hyperpycnal flows and hybrid event beds related to glacial outburst events in a Late Ordovician proglacial delta (Murzuk Basin, SW Libya). *Journal of Sedimentary Research* 82, 688–708.

- Gobo, K., Ghinassi, M. & Nemeč, W. 2014: Reciprocal changes in foreset to bottomset facies in a Gilbert-type delta: response to short-term changes in base level. *Journal of Sedimentary Research* 84, 1079–1095.
- Gobo, K., Ghinassi, M. & Nemeč, W. 2015: Gilbert-type deltas recording short-term base-level changes: delta-brink morphodynamics and related foreset facies. *Sedimentology* 62, 1923–1949.
- Gutsell, J. E., Clague, J. J., Best, M. E., Bobrowsky, P. T. & Hutchinson, I. 2004: Architecture and evolution of a fjord-head delta, western Vancouver Island, British Columbia. *Journal of Quaternary Science* 19, 497–511.
- Harms, J. C., Southard, J. B., Spearing, D. R. & Walker, R. G. 1975: Depositional environments as interpreted from primary sedimentary structures and stratification sequences. *SEPM Short Course Lecture Notes* 2, 1–161.
- Heller, P. L., Paola, C., Hwang, I.-G., John, B. & Steel, R. 2001: Geomorphology and sequence stratigraphy due to slow and rapid base-level changes in an experimental subsiding basin (XES 96-1). *AAPG Bulletin* 85, 817–838.
- Hirst, J. P. P. 2012: Ordovician proglacial sediments in Algeria: insights into the controls on hydrocarbon reservoirs in the In Amenas field, Illizi Basin. In Huuse, M., Redfern, J., Le Heron, D. P., Dixon, R. J., Moscardiello, A. & Craig, J. (eds.): *Glaciogenic Reservoirs*, 319–353. *Geological Society, London, Special Publications* 368.
- Hughes Clarke, J. E. 2016: First wide-angle view of channelized turbidity currents links migrating cyclic steps to flow characteristics. *Nature Communications* 7, Article 118960. Doi: 10.1038/ncomms11896.
- Ilgar, A. & Nemeč, W. 2005: Eraly Miocene lacustrine deposits and sequence stratigraphy of the Ermenk Basin, Central Taurides, Turkey. *Sedimentary Geology* 173, 233–275.
- Jopling, A. V. 1965: Hydraulic factors controlling the shape of lamina in laboratory deltas. *Journal of Sedimentary Petrology* 35, 777–791.
- Juschus, O. 2001: *Das Jungmoränenland südlich von Berlin – Untersuchungen zur jungquartären Landschaftsentwicklung zwischen Unterspreewald und Nuthe*. Ph.D. thesis, Humboldt-Universität zu Berlin, 145 pp.
- Kehe, A. E. & Teller, J. T. 1994: History of Late Glacial runoff along the southwestern margin of the Laurentide Ice Sheet. *Quaternary Science Reviews* 13, 859–877.
- King, R. C., Tingay, M. R. P., Hillis, R. R., Morley, C. K. & Clark, J. 2010: Present-day stress orientations and tectonic provinces of the NW Borneo collisional margin. *Journal of Geophysical Research* 115, B10415, <https://doi.org/10.1029/2009jb006997>.
- Kjær, K. H. & Krüger, J. 2001: The final phase of dead-ice moraine development: processes and sediment architecture, Kötlujökull, Iceland. *Sedimentology* 48, 935–952.
- Kjær, K. H., Larsen, E., van der Meer, J., Ingólfsson, Ó., Krüger, J., Benediktsson, Í. Ó., Knudsen, C. G. & Schomacker, A. 2006: Subglacial decoupling at the sediment/bedrock interface: a new mechanism for rapid flowing ice. *Quaternary Science Reviews* 25, 2704–2712.
- Kneller, B. C. & Branney, M. J. 1995: Sustained high-density turbidity currents and the deposition of thick massive sands. *Sedimentology* 42, 607–616.
- Kostic, S. 2011: Modeling of submarine cyclic steps: controls on their formation, migration, and architecture. *Geosphere* 7, 294–304.
- Kostic, S., Parker, G. & Marr, J. G. 2002: The role of turbidity currents in setting the foreset slope of clinoforms prograding into standing fresh water. *Journal of Sedimentary Research* 72, 353–362.
- Kukkonen, I. T., Olesen, O., Ask, M. V. S. & PFDP Working Group 2010: Postglacial faults in Fennoscandia: targets for scientific drilling. *GFF* 132, 71–81.
- Lang, J. & Winsemann, J. 2013: Lateral and vertical facies relationships of bedforms deposited by aggrading supercritical flows: from cyclic steps to humpback dunes. *Sedimentary Geology* 296, 36–54.
- Lang, J., Brandes, C. & Winsemann, J. 2017a: Erosion and deposition by supercritical density flows during channel avulsion and backfilling: field examples from coarse-grained deepwater channel-levee complexes (Sandino Forearc Basin, southern Central America). *Sedimentary Geology* 349, 79–102.
- Lang, J., Dixon, R. J., Le Heron, D. P. & Winsemann, J. 2012: Depositional architecture and sequence stratigraphic correlation of Upper Ordovician glaciogenic deposits, Illizi Basin, Algeria. In Huuse, M., Redfern, J., Le Heron, D. P., Dixon, R. J., Moscardiello, A. & Craig, J. (eds.): *Glaciogenic Reservoirs*, 293–317. *Geological Society, London, Special Publications* 368.
- Lang, J., Hampel, A., Brandes, C. & Winsemann, J. 2014: Response of salt structures to ice-sheet loading: implications for ice-marginal and subglacial processes. *Quaternary Science Reviews* 101, 217–233.
- Lang, J., Lauer, T. & Winsemann, J. 2018: New age constraints for the Saalian glaciation in northern central Europe: implications for the extent of ice sheets and related proglacial lake systems. *Quaternary Science Reviews* 180, 240–259.
- Lang, J., Sievers, J., Loewer, M., Igel, J. & Winsemann, J. 2017b: 3D architecture of cyclic step and antidune deposits in glaciogenic subaqueous fan and delta settings: integrating outcrop and ground-penetrating radar data. *Sedimentary Geology* 362, 83–100.
- Lee, K., McMechan, G. A., Gani, M. R., Bhattacharya, J. P., Zeng, X. & Howell, C. D. 2007: 3-D architecture and sequence stratigraphic evolution of a forced regressive top-truncated mixed-influenced delta, Cretaceous Wall Creek sandstone, Wyoming, USA. *Journal of Sedimentary Research* 77, 303–323.
- Lehné, R. & Sirocco, F. 2005: Quantification of recent movement potentials in Schleswig-Holstein (Germany) by GIS based calculation of correlation coefficients. *International Journal of Earth Sciences* 94, 1094–1102.
- Longhitano, S. G. 2008: Sedimentary facies and sequence stratigraphy of coarse-grained Gilbert-type deltas within the Pliocene thrust-top Potenza Basin (Southern Apennines, Italy). *Sedimentary Geology* 210, 87–110.
- Lønne, I. 1995: Sedimentary facies and depositional architecture of ice-contact glaciomarine systems. *Sedimentary Geology* 98, 13–43.
- Lønne, I. & Nemeč, W. 2004: High-arctic fan delta recording deglaciation and environment disequilibrium. *Sedimentology* 51, 553–589.
- Macdonald, R. G., Alexander, J., Bacon, J. C. & Cooker, M. J. 2009: Flow patterns, sedimentation and deposit architecture under a hydraulic jump on a non-eroding bed: defining hydraulic-jump unit bars. *Sedimentology* 56, 1346–1367.
- Marren, P. M. 2005: Magnitude and frequency in proglacial rivers: a geomorphological and sedimentological perspective. *Earth-Science Reviews* 70, 203–251.
- Martin, M. & Jansson, K. N. 2011: Glacial geomorphology and glacial lakes of central Transbaikalia, Siberia, Russia. *Journal of Maps* 7, 18–30.
- Martini, I., Ambrosetti, E. & Sandrelli, F. 2017: The role of sediment supply in large-scale stratigraphic architecture of ancient Gilbert-type deltas (Pliocene Siena-Radicofani Basin, Italy). *Sedimentary Geology* 350, 23–41.
- Massari, F. 1996: Upper-flow-regime stratification types on steep-face, coarse-grained, Gilbert-type progradational wedges (Pleistocene, southern Italy). *Journal of Sedimentary Research* 66, 364–375.
- Massari, F. 2017: Supercritical-flow structures (backset-bedded sets and sediment waves) on high-gradient clinoform systems influenced by shallow-marine hydrodynamics. *Sedimentary Geology* 360, 73–95.
- Massari, F. & Parea, G. C. 1990: Wave-dominated Gilbert-type gravel deltas in the hinterland of the Gulf of Taranto (Pleistocene, southern Italy). In Colella, A. & Prior, B. D. (eds.): *Coarse-Grained Deltas*, 311–331. *International Association of Sedimentologists Special Publication* 10.
- McClay, K. R., Dooley, T. & Lewis, G. 1998: Analog modeling of progradational delta systems. *Geology* 26, 771–774.
- McClay, K. R., Dooley, T. & Zamora, G. 2003: Analogue models of delta systems above ductile substrates. In Van Rensbergen, P., Hillis, R. R., Maltman, A. J. & Morley, C. K. (eds.): *Subsurface Sediment Mobilization*, 411–428. *Geological Society, London, Special Publications* 216.
- Meinsen, J., Winsemann, J., Weitkamp, A., Landmeyer, N., Lenz, A. & Dölling, A. 2011: Middle Pleistocene (Saalian) lake outburst floods in the Münsterland Embayment (NW Germany): impacts and magnitudes. *Quaternary Science Reviews* 30, 2597–2625.
- Mitchum, R. M., Vail, P. R. & Sangree, J. B. 1977: Seismic stratigraphy and global changes of sea-level, Part 6: stratigraphic interpretation of seismic reflection patterns in depositional sequences. In Payton, C. E.

- (ed.): *Seismic Stratigraphy – Applications to Hydrocarbon Exploration*, 117–133. *AAPG Memoir* 26.
- Mulder, T. & Alexander, J. 2001: The physical character of subaqueous sedimentary density flows and their deposits. *Sedimentology* 48, 269–299.
- Muto, T. & Steel, R. J. 2001: Autostepping during the transgressive growth of deltas: results from flume experiments. *Geology* 29, 771–774.
- Muto, T. & Steel, R. J. 2004: Autogenic response of fluvial deltas to steady sea-level fall: implications from flume-tank experiments. *Geology* 32, 401–404.
- Muto, T., Yamagishi, C., Sekiguchi, T., Yokokawa, M. & Parker, G. 2012: The hydraulic autogenesis of distinct cyclicity in delta foreset bedding: flume experiments. *Journal of Sedimentary Research* 82, 545–558.
- Neal, A. 2004: Ground-penetrating radar and its use in sedimentology: principles, problems and progress. *Earth-Science Reviews* 66, 261–330.
- Nemec, W. 1990: Aspects of sediment movement on steep delta slopes. In Colella, A. & Prior, B. D. (eds.): *Coarse-Grained Deltas*, 29–73. *International Association of Sedimentologists Special Publication* 10.
- Nemec, W., Lønne, I. & Blikra, L. H. 1999: The Kregnes moraine in Gaudalen, west-central Norway: anatomy of a Younger Dryas proglacial delta in a paleofjord basin. *Boreas* 28, 454–476.
- Nutz, A., Ghiene, J. F., Schuster, M., Dietrich, P., Roquin, C., Hay, M. B., Bouchette, F. & Cousineau, P. A. 2015: Forced regressive deposits of a deglaciation sequence: example from the Late Quaternary succession in the Lake Saint-Jean basin (Québec, Canada). *Sedimentology* 62, 1573–1610.
- Olariu, C. & Bhattacharya, J. P. 2006: Terminal distributary channels and delta front architecture of river-dominated delta systems. *Journal of Sedimentary Research* 76, 212–233.
- Oviatt, C. G., Currey, D. R. & Sack, D. 1992: Radiocarbon chronology of Lake Bonneville, Eastern Great Basin, USA. *Palaeogeography, Palaeoclimatology, Palaeoecology* 99, 225–241.
- Owen, G. 1996: Experimental soft-sediment deformation: structures formed by the liquefaction of unconsolidated sands and some ancient examples. *Sedimentology* 43, 279–293.
- Perkins, A. J. & Brennand, T. A. 2015: Refining the pattern and style of Cordilleran Ice Sheet retreat: palaeogeography, evolution and implications of lateglacial ice-dammed lake systems on the southern Fraser Plateau, British Columbia, Canada. *Boreas* 44, 319–342.
- Petter, A. L. & Muto, T. 2008: Sustained alluvial aggradation and autogenic detachment of the alluvial river from the shoreline in response to steady fall of relative sea-level. *Journal of Sedimentary Research* 78, 98–111.
- Plink-Björklund, P. & Ronnert, L. 1999: Depositional processes and internal architecture of late Weichselian ice-margin submarine fan and delta settings, Swedish west coast. *Sedimentology* 46, 215–234.
- Plink-Björklund, P. & Steel, R. J. 2004: Initiation of turbidity currents: outcrop evidence of hyperpycnal flow turbidites. *Sedimentary Geology* 165, 29–52.
- Poppe, S., Holohan, E. P., Pauwels, E., Cnudde, V. & Kervyn, M. 2015: Sinkholes, pit craters, and small calderas: analog models of depletion induced collapse analyzed by computed X-ray microtomography. *Geological Society of America Bulletin* 127, 281–296.
- Porębski, S. J. & Steel, R. J. 2006: Deltas and sea-level change. *Journal of Sedimentary Research* 76, 390–403.
- Posamentier, H. W. & Morris, W. R. 2000: Aspects of the stratal architecture of forced regressive deposits. In Hunt, D. & Gawthorpe, R. L. (eds.): *Sedimentary Responses to Forced Regressions*, 19–46. *Geological Society, London, Special Publications* 172.
- Posamentier, H. W. & Vail, P. R. 1988: Eustatic controls on clastic deposition II – Sequence and system tract models. In Wilgus, C. K., Hastings, B. J., Posamentier, H. W., Van Wagoner, J. C., Ross, C. A. & Kendall, C. G. S. C. (eds.): *Sea-Level Changes – An Integrated Approach*, 125–154. *SEPM Special Publication* 42.
- Postma, G. 1990: Depositional architecture and facies of river and fan deltas: a synthesis. In Colella, A. & Prior, B. D. (eds.): *Coarse-Grained Deltas*, 13–27. *International Association of Sedimentologists Special Publication* 10.
- Postma, G. 1995: Sea-level-related architectural trends in coarse-grained delta complexes. *Sedimentary Geology* 98, 3–12.
- Postma, G. & Cartigny, M. J. B. 2014: Supercritical and subcritical turbidity currents and their deposits – a synthesis. *Geology* 42, 987–990.
- Postma, G., Cartigny, M. J. B. & Kleverlaan, K. 2009: Structureless, coarse-tail graded Bouma Ta formed by internal hydraulic jump of the turbidity current? *Sedimentary Geology* 219, 1–6.
- Postma, G., Kleverlaan, K. & Cartigny, M. J. B. 2014: Recognition of cyclic steps in sandy and gravelly turbidite sequences, and consequences for the Bouma facies model. *Sedimentology* 61, 2268–2290.
- Powell, R. D. 1990: Glacimarine processes at grounding-line fans and their growth to ice-contact deltas. In Dowdeswell, J. A. & Scourse, J. D. (eds.): *Glacimarine Environments: Processes and Sediment*, 53–73. *Geological Society, London, Special Publications* 53.
- Powell, R. D. & Cooper, J. M. 2002: A glacial sequence stratigraphic model for temperate, glaciated continental shelves. In Dowdeswell, J. A. & Ó Cofaigh, C. (eds.): *Glacier-Influenced Sedimentation on High-Latitude Continental Margins*, 215–244. *Geological Society, London, Special Publications* 203.
- Prange, W. 1995: Kleintektonische Untersuchungen in Lockersedimenten. *Schriften des Naturwissenschaftlichen Vereins für Schleswig-Holstein* 65, 47–65.
- Ritchie, B. D., Gawthorpe, R. L. & Hardy, S. 2004a: Three-dimensional numerical modelling of deltaic depositional sequences 1: influence of the rate and magnitude of sea-level change. *Journal of Sedimentary Research* 74, 203–220.
- Ritchie, B. D., Gawthorpe, R. L. & Hardy, S. 2004b: Three-dimensional numerical modelling of deltaic depositional sequences 2: influence of local controls. *Journal of Sedimentary Research* 74, 221–238.
- Roskosch, J., Winsemann, J., Polom, U., Brandes, C., Tsukamoto, S., Weitkamp, A., Bartholomäus, W. A., Henningsen, D. & Frechen, M. 2015: Luminescence dating of ice-marginal deposits in northern Germany: evidence for repeated glaciations during the Middle Pleistocene (MIS 12 to MIS 6). *Boreas* 44, 103–126.
- Selsing, L. 1981: Stress analysis on conjugate normal faults in unconsolidated Weichselian glacial sediments from Brorfelde, Denmark. *Boreas* 10, 275–279.
- Sohn, Y. K. & Son, M. 2004: Synrift stratigraphic geometry in a transfer zone coarse-grained delta complex, Miocene Pohang Basin, SE Korea. *Sedimentology* 51, 1387–1408.
- Sohn, Y. K., Kim, S. B., Hwang, I. G., Bahk, J. J., Choe, M. Y. & Chough, S. K. 1997: Characteristics and depositional processes of large-scale gravelly Gilbert-type foresets in the Miocene Dousan fan delta, Pohang Basin, SE Korea. *Journal of Sedimentary Research* 67, 130–141.
- Strong, N. & Paola, C. 2008: Valleys that never were: time surfaces versus stratigraphic surfaces. *Journal of Sedimentary Research* 78, 579–593.
- Talling, P. J. 2014: On the triggers, resulting flow types and frequencies of subaqueous sediment density flows in different settings. *Marine Geology* 352, 155–182.
- Teller, J. T. 1987: Proglacial lakes and the southern margin of the Laurentide Ice Sheet. In Ruddiman, W. F. & Wright, H. E. (eds.): *North America and Adjacent Oceans During the Last Deglaciation. The Decade of North American Geology*, 39–69. *Geological Society of America K3*.
- Tylmann, K., Piotrowski, J. A. & Wysota, W. 2012: The ice/bed interface mosaic: deforming spots intervening with stable areas under the fringe of the Scandinavian Ice Sheet at Samplawa, Poland. *Boreas* 42, 428–441.
- Uličný, D. 2001: Depositional systems and sequence stratigraphy of coarse-grained deltas in a shallow-marine, strike-slip setting: the Bohemian Cretaceous Basin, Czech Republic. *Sedimentology* 48, 599–628.
- Ventra, D., Cartigny, M. J. B., Bijkerk, J. F. & Acikalin, S. 2015: Supercritical-flow structures on a Late Carboniferous delta front: sedimentological and paleoclimatic significance. *Geology* 43, 731–734.
- Villiers, G., Kleinhans, M. G. & Postma, G. 2013: Experimental delta formation in crater lakes and implications for interpretation of Martian deltas. *Journal of Geophysical Research Planets* 118, 651–670.
- Walker, R. G. 1975: Conglomerates: sedimentary structures and facies models. In Harms, J. C., Walker, R. G. & Spearing, D. (eds.):

- Depositional Environments as Interpreted from Primary Sedimentary Structures and Stratification Sequences*, 133–161. *SEPM Short Course Lecture Notes 12*.
- Winsemann, J., Alho, P., Laamanen, L., Goseberg, N., Lang, J. & Klostermann, J. 2016: Flow dynamics, sedimentation and erosion of glacial lake outburst floods along the Middle Pleistocene Scandinavian ice sheet (northern Central Europe). *Boreas* 45, 260–283.
- Winsemann, J., Aspiron, U., Meyer, T. & Schramm, C. 2007: Facies characteristics of Middle Pleistocene (Saalian) ice-margin subaqueous fan and delta deposits, glacial Lake Leine, NW Germany. *Sedimentary Geology* 193, 105–129.
- Winsemann, J., Brandes, C. & Polom, U. 2011: Response of a proglacial delta to rapid high-amplitude lake level change: an integration of outcrop data and high resolution shear wave seismic. *Basin Research* 23, 22–52.
- Winsemann, J., Hornung, J. J., Meinsen, J., Aspiron, U., Polom, U., Brandes, C., Bußmann, M. & Weber, C. 2009: Anatomy of a subaqueous ice-contact fan and delta complex, Middle Pleistocene, NW Germany. *Sedimentology* 36, 1041–1076.
- Wright, L. D. 1977: Sediment transport and deposition at river mouths: a synthesis. *Geological Society of America Bulletin* 88, 857–868.
- Zhong, G., Cartigny, M. J. B., Kuang, Z. & Wang, L. 2015: Cyclic steps along the South Taiwan Shoal and West Penghu submarine canyons on the northeastern continental slope of the South China Sea. *Geological Society of America Bulletin* 127, 804–824.